F_4, E_6 and G_2 exceptional gauge groups in the vacuum domain structure model

Amir Shahlaei* and Shahnoosh Rafibakhsh†

Department of Physics, Science and Research Branch, Islamic Azad University, Tehran 14665/678, Iran

(Received 4 December 2017; published 21 March 2018)

Using a vacuum domain structure model, we calculate trivial static potentials in various representations of F_4, E_6, and G_2 exceptional groups by means of the unit center element. Due to the absence of the nontrivial center elements, the potential of every representation is screened at far distances. However, the linear part is observed at intermediate quark separations and is investigated by the decomposition of the exceptional group to its maximal subgroups. Comparing the group factor of the supergroup with the corresponding one obtained from the nontrivial center elements of $SU(3)$ subgroup shows that $SU(3)$ is not the direct cause of temporary confinement in any of the exceptional groups. However, the trivial potential obtained from the group decomposition into the $SU(3)$ subgroup is the same as the potential of the supergroup itself. In addition, any regular or singular decomposition into the $SU(2)$ subgroup that produces the Cartan generator with the same elements as h_1, in any exceptional group, leads to the linear intermediate potential of the exceptional gauge groups. The other $SU(2)$ decompositions with the Cartan generator different from h_1 are still able to describe the linear potential if the number of $SU(2)$ nontrivial center elements that emerge in the decompositions is the same. As a result, it is the center vortices quantized in terms of nontrivial center elements of the $SU(2)$ subgroup that give rise to the intermediate confinement in the static potentials.

DOI: 10.1103/PhysRevD.97.056015

I. INTRODUCTION AND MOTIVATION

Quantum chromodynamics is the theory of strong interactions. Quarks interact via gluons that are strong force carriers and are attributed to the adjoint representation of the $SU(3)$ gauge group. The non-Abelian nature of gluons causes QCD to be fundamentally a nonperturbative theory in the infrared sector. To understand the phenomena of the low energy regime, such as confinement, some topological field configurations, such as center vortices [1–15], are believed to play the key role in the nontrivial vacuum of QCD. They assign a criterion to confinement through the area-law falloff of the Wilson loop, which is one of the most efficient order parameters for investigating the large distance behavior of QCD.

In the center vortex model, confinement is the result of the interaction between center vortices and the Wilson loop. In fact, the Wilson loop running around the vortex measures the vortex flux, which is quantized in terms of the gauge group center. A center vortex, which is topologically linked to a Wilson loop, changes the Wilson loop by a group factor z_n:

$$W(C) \to (z_n)^k W(C), \tag{1}$$

where $z_n = \exp(\frac{2\pi i n}{N})$, $n = 1, 2, \ldots, N-1$, and k represents the N-ality of the representation r. This property implies a linear potential between static quarks, which means confinement.

The thick center vortex model developed by Faber *et al.* [16] is aimed at studying the potentials of higher representations of $SU(N)$ gauge groups. In this model, the quark-antiquark static potential behaves differently in three regions. At short distances, the interaction is determined by one-gluon exchange, which leads to a Coulomb-like potential [17–19]. At intermediate distances, the string tension of the linear potential is proportional to Casimir scaling. In the asymptotic region, potentials of all representations with zero N-ality are screened. However, the potential of nonzero N-ality representations becomes parallel to the one of the lowest representation with the same N-ality [16,20–23].

In 2007, Greensite *et al.* [24] claimed that there is no obvious reason to exclude the trivial center element from the model. In fact, even in G_2 gauge theory, which only includes one trivial center element, one expects a linear potential from the breakdown of the perturbation theory to

*amirshahlaei@gmail.com
†Corresponding author.
rafibakhsh@srbiau.ac.ir

the onset of screening while all asymptotic string tensions are zero. Monte Carlo numerical lattice calculations for G_2 [25–27] also confirm a confining potential, despite the absence of nontrivial center elements. In the new model, a vacuum domain is a closed tube of magnetic flux that, unlike a vortex, is quantized in units corresponding to the gauge group trivial center. The string tensions are produced from random spatial variations of the color magnetic flux quantized in terms of unity. But, what accounts for the intermediate linear potential in such gauge groups? To answer this question and by using the idea of domain structures, Deldar *et al.* [28–30] showed that $SU(2)$ and $SU(3)$ subgroups of G_2 have an important role in the intermediate confinement of G_2. In fact, they were motivated by the two works in Refs. [24,31]. Holland *et al.* [31] investigated that a scalar Higgs field in the fundamental representation of G_2 can break to $SU(3)$ representations. So, one is able to interpolate between exceptional and ordinary confinement. Moreover, Greensite *et al.* [24] used the Abelian dominance idea to study $SU(3)$ and $SU(2)$ dominance in the G_2 gauge theory. Therefore, it seems interesting to investigate how confinement appears in a theory with exceptional gauge groups in the framework of the vacuum domain structure model.

In this paper, using the same method as in Refs. [28–30], we present a general scheme to understand what kind of group decompositions lead to the temporary confinement of the exceptional gauge groups in the vacuum domain structure model. In the next section, the thick center vortex and vacuum domain structure models are discussed briefly. In Sec. III, some properties of exceptional groups are investigated. We apply F_4, E_6, and G_2 in the vacuum domain structure model and calculate the potentials in different representations in Sec. IV. The decomposition of these gauge groups into their subgroups is investigated as well.

II. THICK CENTER VORTEX MODEL AND VACUUM DOMAIN STRUCTURES

A center vortex is a closed tube of magnetic flux that is quantized in terms of the nontrivial center elements of the gauge group. It might be considered as linelike (in three dimensions) or as a surfacelike (in four dimensions) object. In a pure non-Abelian gauge theory, the random fluctuations in the number of center vortices that pierce the minimal area of the Wilson loop give rise to the asymptotic string tension. In fact, a thin center vortex is capable of inducing the linear potential for the fundamental representation of the gauge group. Thickening the center vortices leads to a bigger piercing area and these topological objects should be described by a profile function. Therefore, the gauge group centers in Eq. (1) should be replaced by a group factor,

$$W(C) \to \mathcal{G}_r[\vec{\alpha}_C^n]W(C), \tag{2}$$

where the group factor is described as

$$\mathcal{G}_r[\vec{\alpha}_C^n(x)] = \frac{1}{d_r}\mathrm{Tr}[\exp(i\vec{\alpha}_C^n \cdot \vec{H})], \tag{3}$$

in which d_r depicts the dimension of the group representation; H_i, $i = 1, \ldots, N-1$, are simultaneous diagonal generators of the group spanning the Cartan subalgebra; and n represents the type of center vortex. Vortices of type n and type $N-n$ are complex conjugates of each other and their magnetic fluxes are in the opposite directions. Therefore,

$$\mathcal{G}_r[\vec{\alpha}_C^n(x)] = \mathcal{G}_r^*[\vec{\alpha}_C^{N-n}(x)]. \tag{4}$$

The function $\vec{\alpha}_C^n(x)$ is the vortex profile ansatz. It depends on the location of the vortex midpoint x, from the Wilson loop, the shape of the contour C, and the vortex type n. Mathematically, there are various candidates that can simulate a well-defined potential, but all of them should obey the following conditions:

(1) As $R \to 0$, then $\alpha \to 0$.
(2) When the vortex core lies entirely outside the minimal planar area enclosed by the Wilson loop, there is no interaction:

$$\exp[i\vec{\alpha}_C^n \cdot \vec{H}] = \mathbb{I} \Rightarrow \vec{\alpha}_C^n = 0. \tag{5}$$

(3) Whenever the vortex core is completely inside the planar area of the Wilson loop,

$$\exp[i\vec{\alpha}_C^n \cdot \vec{H}] = z_n\mathbb{I} \Rightarrow \vec{\alpha}_C^n = \vec{\alpha}_{\max}^n. \tag{6}$$

Here, we have chosen the flux profile introduced in Ref. [16]:

$$\vec{\alpha}_C^n(x) = \frac{\vec{\alpha}_{\max}^n}{2}\left[1 - \tanh\left(ay(x) + \frac{b}{R}\right)\right], \tag{7}$$

where a and b are free parameters of the model. The distance between the vortex midpoint and the nearest timelike leg of the Wilson loop is measured by $y(x)$:

$$y(x) = \begin{cases} x - R & \text{for } |R - x| \le |x| \\ -x & \text{for } |R - x| > |x| \end{cases}. \tag{8}$$

It seems changing the ansatz may have no effect on the extremum points of the group factor $\mathcal{G}_r[\vec{\alpha}(x)]$ [32], whereas an alteration of $\vec{\alpha}_C^n(x)$ is influential in the potential itself in a way that string tension ratios might be more or less in agreement with Casimir scaling [21,30].

Now we are able to write the Wilson loop for $SU(N)$ gauge groups:

$$\langle W(C)\rangle = \prod_x\left(1 - \sum_{n=1}^{N-1} f_n(1 - \mathcal{G}_r[\vec{\alpha}_C^n(x)])\right)\langle W_0(C)\rangle, \tag{9}$$

where f_n shows the probability that the midpoint of a center vortex is located at any plaquette in the plane of the Wilson loop. The probability of locating center vortices of any type at any two plaquettes is independent, which is an oversimplification of the model. $\langle W_0(C)\rangle$ is the Wilson loop expectation value when no vortices are linked with the loop. It should be noted that in addition to the regions associated with the nontrivial center elements, the domains corresponding to unity center elements are also allowed in the vacuum. Therefore, the sum in Eq. (9) should contain $n=0$ as well. Using the fact that $f_n = f_{N-n}$, the static potential between a color and an anticolor source induced by thick center vortices and vacuum domains is

$$V(R) = -\sum_{m=-\infty}^{m=+\infty} \ln\left\{1 - \sum_{n=0}^{N-1} f_n(1 - \mathrm{Re}\mathcal{G}_r[\vec{\alpha}_C^n(x_m)])\right\}, \tag{10}$$

where $n=0$ denotes a vacuum domain type vortex and $n = 1, \ldots, N-1$ indicates the type of center vortex.

III. SOME PROPERTIES OF EXCEPTIONAL GROUPS

The ideas of symmetries and Lie exceptional groups have always been attractive in modern high energy physics. G_2 is the simplest exceptional gauge group that confirms the chance of having confinement without the center [31]. G_2 gauge theory is a theoretical laboratory in which $SU(N)$ subgroups are embedded. This provides us with an understanding not only about the exceptional G_2 confinement but also about the $SU(3)$ confinement that happens in nature. In this section, we briefly explain some properties of the exceptional groups applied in this article, including their subgroups and Dynkin diagrams.

In general, there are five distinguishable exceptional groups named G_2, F_4, E_6, E_7, and E_8. The subscripts point out the ranks of the groups. The numbers of simple roots and simultaneous diagonal generators of simple Lie groups are equivalent to their rank. One may draw the whole root diagram by having simple roots and the angles between them in a simple Lie group. The angle between simple roots in a Dynkin diagram is always obtuse. Three, two, one or no lines between simple roots measure their mid angles, which are 150°, 135°, 120°, or 90°, respectively [33]. Figure 1 depicts Dynkin diagrams of the exceptional groups used in this research. Filled circles represent shorter roots and empty ones show longer roots in terms of their length.

Using Dynkin diagrams, one is able to find the subgroups of every lie group. There are three different sorts of maximal subgroups [34]:

(i) Regular maximal nonsemisimple subgroups,
(ii) Regular maximal semisimple subgroups,
(iii) Singular (special) maximal subgroups.

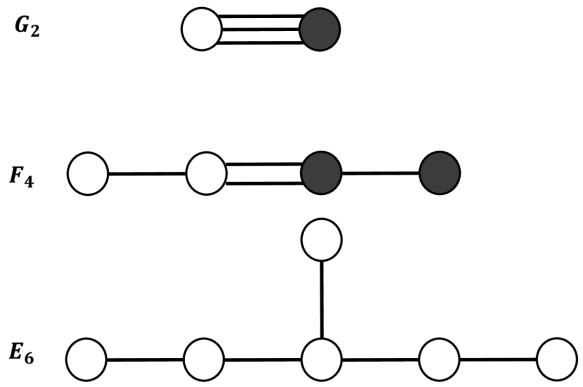

FIG. 1. Dynkin diagrams of G_2, F_4, and E_6 exceptional groups.

The sum of the ranks of the regular subgroups is equal to the rank of their supergroup. However, this is not true for the singular subgroups. It should be noted that if a factor $U(1)$ appears in a subgroup, it makes the subgroup as a nonsemisimple one.

In this article, we briefly discuss how to derive the subgroups of F_4 and use the same method for other exceptional groups. The extended Dynkin diagram is structured by adding the most negative root $(-\gamma)$ to the set of simple roots (Fig. 2). Then, by omitting the original β_i roots, regular subgroups will emerge one by one. For example, in Fig. 2, eliminating the root β_2 leads to the $SU(3)\times SU(3)$ subgroup of F_4. Moreover, when the root β_4 is omitted, the $SO(9)$ subgroup of F_4 is obtained. It should be pointed out that omitting the root β_3 gives off the $SU(2)\times SU(4)$ subgroup. In some references, it has been claimed as a direct subgroup of F_4 [35] and in some others it is not [36,37]. However, it is a direct subgroup of $SO(9)$. Therefore, it might be, at least, considered as an indirect subgroup of F_4. To achieve singular maximal subgroups of exceptional groups, a determined method does not exist and each subgroup has to be extracted individually [34]. All maximal subgroups of the F_4 exceptional group have been presented in Table I.

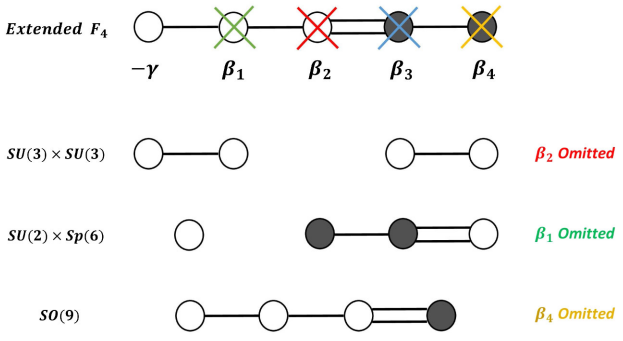

FIG. 2. Three different regular maximal subgroups of F_4 obtained from its extended Dynkin diagram by omitting the original simple roots one by one.

TABLE I. Maximal subgroups of some exceptional groups [37]. [R] and [S] represent regular and singular subgroups of each group, respectively.

E_6	F_4	G_2
$SU(3)\times SU(3)\times SU(3)$ [R]	$SU(3)\times SU(3)$ [R]	$SU(3)$ [R]
$SU(2)\times SU(6)$ [R]	$SU(2)\times Sp(6)$ [R]	$SU(2)\times SU(2)$ [R]
$SO(10)\times U(1)$ [R]	$SO(9)$ [R]	$SU(2)$ [S]
$SU(3)\times G_2$ [S]	$SU(2)\times G_2$ [S]	
$SU(3)$ [S]	$SU(2)$ [S]	
$Sp(8)$ [S]		
G_2 [S]		
F_4 [S]		

Based on the branching rules, an irreducible representation of a group can be decomposed into the irreps of its subgroup as follows [36]:

$$R(G) = \bigoplus_i m_i R_i(g), \tag{11}$$

where $R(G)$ is an irrep of the supergroup G and $R_i(g)$ is the irrep of the subgroup g. m_i is the degeneracy of the representation $R_i(g)$ in the decomposition of representation 36,37] $R(G)$]. To be more precise, we consider one of the regular subgroups of F_4:

$$F_4 \supset SU(3)\times SU(3).$$

Using the branching rules, one might write [36–38]

$$26 = (8,1)\oplus(3,3)\oplus(\bar{3},\bar{3}). \tag{12}$$

From Eq. (11), it is obvious that the first numbers in each parenthesis could be considered as the degeneracy of the second representation emerging in the decomposition:

$$26 = 8(1) + 3(3) + 3(\bar{3}). \tag{13}$$

Therefore, an F_4 "quark" is made up of three $SU(3)$ quarks, three antiquarks, and one singlet.

IV. CONFINEMENT WITHOUT A CENTER

A. F_4 exceptional group

The F_4 exceptional group has rank four and contains four Cartan generators. The diagonal generators for the fundamental 26-dimensional representation of F_4 are [39,40]

$$\begin{aligned}
h_1 &= N_1(D_5^5 + D_6^6 - D_7^7 + D_8^8 - D_9^9 - D_{10}^{10}),\\
h_2 &= N_2(D_3^3 + D_4^4 - D_5^5 - D_6^6 + D_{10}^{10} - D_{11}^{11}),\\
h_3 &= \frac{N_3}{2}(D_2^2 - 2D_3^3 - D_4^4 + D_6^6 - D_8^8 + D_9^9\\
&\quad - D_{10}^{10} + D_{11}^{11} - D_{12}^{12}),\\
h_4 &= \frac{N_4}{2}(-2D_2^2 + D_3^3 - D_4^4 + D_5^5 - D_6^6 + D_7^7\\
&\quad - D_9^9 + D_{12}^{12} - D_{13}^{13}),
\end{aligned} \tag{14}$$

where

$$D_a^b = I_{ab} - I_{\bar{b}\bar{a}}, \tag{15}$$

and I_{ab} are 26×26 matrices with the following matrix elements:

$$(I_{ab})_{jk} = \delta_{aj}\delta_{bk}. \tag{16}$$

Subscripts j and k take on the same values as a and b such that a, b: $-13 \le j,\ k \le 13$ with zero excluded.

Using the standard normalization condition

$$\mathrm{Tr}[h_a, h_b] = \frac{1}{2}\delta_{ab}, \tag{17}$$

we calculate the normalization factors as follows:

$$\begin{aligned}
N_1 &= N_2 = \frac{1}{2\sqrt{6}},\\
N_3 &= N_4 = \frac{1}{2\sqrt{3}}.
\end{aligned} \tag{18}$$

To find the maximum amount of the domain structure flux, we use Eq. (6), using the fact that the F_4 gauge group includes only one trivial center element,

$$\exp[i\vec{\alpha}\cdot\vec{H}] = \mathbb{I}, \tag{19}$$

and we find

$$\begin{aligned}
\alpha_1^{\max} &= 2\pi\sqrt{24},\\
\alpha_2^{\max} &= 6\pi\sqrt{24},\\
\alpha_3^{\max} &= 4\pi\sqrt{48},\\
\alpha_4^{\max} &= 2\pi\sqrt{48}.
\end{aligned} \tag{20}$$

Now, one can calculate the static potential of Eq. (10) for the fundamental representation of the F_4 exceptional gauge group. This potential has been pictured in Fig. 3 for $R \in [1, 100]$. The free parameters of the model are chosen to be $a = 0.05$, $b = 4$, and $f = 0.1$ in every calculation of this article.

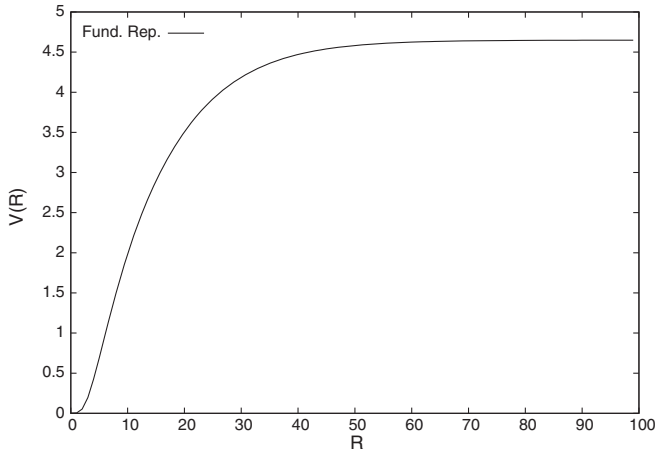

FIG. 3. The potential between two static sources in the fundamental representation of F_4 for $R \in [1, 100]$. Screening is clearly observed at large quark separations while the potential is linear at intermediate distances. The free parameters of the model have been chosen to be $a = 0.05$, $b = 4$, and $f = 0.1$.

In Fig. 3, the linear potential is demonstrably located in the approximate range of $R \in [2, 9]$. In addition, at large distances where the vacuum domain is entirely located inside of the Wilson loop, a flat potential is induced. Hence, one can deduce that in groups without a nontrivial center, static potentials of all representations behave like a $SU(N)$ representation with zero N-ality.

The adjoint representation of F_4 is 52 dimensional. As a consequence, like any gauge group, the "bosonic gluons" of the F_4 exceptional group are made of the adjoint representation. Thus, mathematically one can derive the way of screening of color sources in any representation from tensor products of that representation with the adjoint one; i.e., when a singlet emerges, it means screening. So, for the fundamental representation, one may write

$$26 \times 52 = 26 \oplus 273 \oplus 1053. \tag{21}$$

Therefore, the fundamental representation of F_4 cannot be screened just by one set of "gluons". Energetically speaking, color sources in the fundamental representation of F_4 are not screened until the potential reaches that extent where four sets of "gluons" pop out of the vacuum:

$$26 \times \overbrace{52 \times \cdots \times 52}^{4 \text{ times}} = \mathbf{1} \oplus 46(26) \oplus 10(52) \oplus \cdots. \tag{22}$$

These tensor products have been calculated by the LieART project in Mathematica [41]. The numbers out of the parentheses are the degeneracy of the representations being repeated in the tensor product. Therefore, four F_4 "gluons" are able to screen an F_4 "quark" to create a color singlet hybrid $qGGGG$. Moreover, two "quarks" form a singlet.

$$26 \times 26 = 1 \oplus 26 \oplus 52 \oplus 273 \oplus 324. \tag{23}$$

As in $SU(N)$ gauge groups, three F_4 "quarks" can create a baryon:

$$26 \times 26 \times 26 = 1 \oplus 5(26) \oplus 2(52) \oplus 4(273) \oplus 3(324) \oplus 3(1053) \oplus 1274 \oplus 2652 \oplus 2(4096). \tag{24}$$

Evidently, the function $\mathrm{Re}\mathcal{G}_r[\vec{\alpha}_C^n(x)]$ looks predominant in the potential formula in Eq. (10). It shows that the group factor varies between 1 and $\exp(\frac{2\pi i n k}{N})$, corresponding to the N-ality=k of the representation and the vortex type n. An unaffected Wilson loop that has not been pierced by any vortex means $\mathrm{Re}\mathcal{G}_r[\vec{\alpha}_C^n(x)] = 1$. When the vortex is linked to the Wilson loop, the group factor deviates from 1. Hence, to investigate what happens to the F_4 potentials, one may study the behavior of the group factor.

In Ref. [32], it has been proven that the third Cartan generator of the $SU(4)$ gauge group, i.e., $H_3 = \frac{1}{2\sqrt{6}}\mathrm{diag}[1, 1, 1, -3]$, can produce the total potential individually. In the F_4 exceptional group, one might use only h_1 or h_2 Cartan generators or both of them together to find the same group factor and also the same potential as if we apply all four Cartan generators in our calculations. This property will be helpful in the decomposition of the F_4 representations into its subgroups. In fact, when the identical diagonal generators are constructed, the same potentials as the F_4 itself will be achieved.

In Fig. 4, the real part of the group factor versus the location x of the vacuum domain midpoint has been plotted, for $R = 100$ and in the range $x \in [-200, 300]$, by

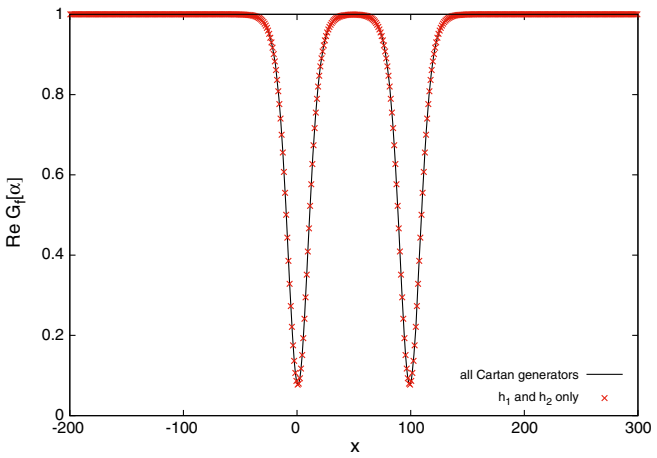

FIG. 4. The real part of the group factor versus x, the location of the vacuum domain midpoint, for the fundamental representation of the F_4 exceptional gauge group in the range $x \in [-200, 300]$, by applying h_1 and h_2 Cartan generators (stars) and all diagonal generators (solid line). It is clear that the two sets of data are the same. The distance R between color and anticolor sources is equal to 100.

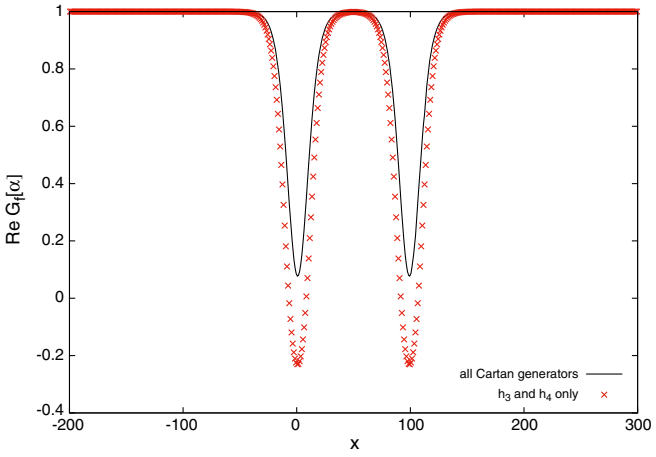

FIG. 5. The same as Fig. 4 but in comparison with the group factor when only h_3 or h_4 is used.

considering all generators and also by utilizing only h_1 and h_2. It is clear that both diagrams in Fig. 4 are identical and the group factor reaches the minimum amount of ≈ 0.076 at $x = 0$ and $x = 100$. To confirm our conclusion, we have plotted a similar diagram in Fig. 5 but by using only h_3 or h_4 diagonal generators. In this figure, the group factor reaches the minimum amount equal to ≈ -0.23, which is way less than the minimum amount of the F_4 group factor.

It has been shown that [32] the group factor reaches the minimum points where 50% of the vortex maximum flux enters the Wilson loop. These points are responsible for the intermediate linear potential. We aim to show that the $SU(N)$ subgroups of the exceptional groups might be the reason for the appearance of the linear potential at intermediate distances. It means that the minimum points of the group factor could be explained by the group decomposition into the subgroups.

1. $SU(3) \times SU(3)$ decomposition

Using the decomposition in Eq. (13), we are able to reconstruct Cartan generators of F_4 with respect to its $SU(3)$ subgroup,

$$H_a^{26} = \frac{1}{\sqrt{6}}\mathrm{diag}[\overbrace{0,\ldots,0}^{8\ \text{times}}, \lambda_a^3, \lambda_a^3, \lambda_a^3, -(\lambda_a^3)^*, -(\lambda_a^3)^*, -(\lambda_a^3)^*], \tag{25}$$

where λ_a^3, $a = 3, 8$ are Cartan generators of $SU(3)$ in the fundamental representation:

$$\lambda_3^3 = \frac{1}{2}\mathrm{diag}[1,-1,0],$$
$$\lambda_8^3 = \frac{1}{2\sqrt{3}}\mathrm{diag}[1,1,-2]. \tag{26}$$

Meanwhile, the matrices of Eq. (25) are normalized using the normalization conditions in Eq. (17). If the matrix H_3^{26} in Eq. (25) is considered, its components are identical to the ones for the Cartan generators h_1 and h_2 of Eq. (14). But this is not the case with H_8^{26}. To examine the results coming out of these two matrices, one is supposed to establish the same normalization condition as in Eq. (19):

$$\exp(i\alpha_{\max_1}^{26} H_3^{26} + i\alpha_{\max_2}^{26} H_8^{26}) = \mathbb{I}. \tag{27}$$

In this case, we have six distinctive equations and find

$$\alpha_{\max_1}^{26} = 2\pi\sqrt{6},$$
$$\alpha_{\max_2}^{26} = 6\pi\sqrt{2}. \tag{28}$$

Now, the potential of Eq. (10) could be calculated using Eqs. (25) and (28). This potential is identical to the one in Fig. 3, despite the difference between H_8^{26} and h_1 or h_2. To investigate this matter, one might manually estimate the value of $\mathrm{Re}\mathcal{G}_r[\alpha]$ when the vacuum domain is completely inside the Wilson loop:

$$\mathrm{Re}\mathcal{G}_r^1[\alpha]_{SU_3\times SU_3} = \frac{1}{26}\times \mathrm{Re}(\mathrm{Tr}[\exp(i\alpha_{\max_1}^{26}\cdot H_3^{26})]) \approx 0.076 \tag{29}$$

$$\mathrm{Re}\mathcal{G}_r^2[\alpha]_{SU_3\times SU_3} = \frac{1}{26}\times \mathrm{Re}(\mathrm{Tr}[\exp(i\alpha_{\max_2}^{26}\cdot H_8^{26})]) \approx 0.076. \tag{30}$$

It is clear that both group factor functions earned by either $\alpha_{\max_1}^{26}$ or $\alpha_{\max_2}^{26}$ reach the same amount, which is the minimum amount of the F_4 group factor in Fig. 4 as well. Consequently, based on the analogy of the group factor functions acquired by both H_3^{26} and H_8^{26}, we claim that, although the second matrix of $SU(3) \times SU(3)$ has different components, it has the same effect as the Cartan h_1 on the F_4 group. Then, the trivial static potential of the F_4 exceptional group is similar to the potential gained by its $SU(3) \times SU(3)$ subgroup. Therefore, it seems that this decomposition could be generalized for higher representations to find the corresponding potential.

The decomposition of the 52-dimensional adjoint representation of the F_4 is [36–38]

$$52 = (8,1) \oplus (1,8) \oplus (\bar{6},3) \oplus (6,\bar{3}),$$
$$52 = 8(1) + 1(8) + 6(3) + 6(\bar{3}). \tag{31}$$

This shows that F_4 "gluons" are made of the usual $SU(3)$ gluons (representation 8) and some additional gluons consist of $SU(3)$ quarks (representation 3) and antiquarks (representation $\bar{3}$) and also eight singlets. It is clear that these representations have different trialities.

Using Eq. (31), the Cartan generators of F_4 in the adjoint representation might be reconstructed as follows:

$$H_a^{52} = \frac{1}{\sqrt{18}}\mathrm{diag}[\overbrace{0,\ldots,0}^{8\ \text{times}}, \lambda_a^8, \overbrace{\lambda_a^3,\cdots\lambda_a^3}^{6\ \text{times}}, \overbrace{-(\lambda_a^3)^*,\ldots,-(\lambda_a^3)^*}^{6\ \text{times}}], \tag{32}$$

where λ_a^3, $a = 3, 8$, are the same generators as in Eq. (26) and λ_a^8 are simultaneous diagonal generators of the $SU(3)$ gauge group in the adjoint eight-dimensional representation. Using Eq. (19), the maximum values of the vortex flux for the adjoint representation of the $F_4 \supset SU(3) \times SU(3)$ decomposition are

$$\alpha_{\max_1}^{52} = 6\pi\sqrt{2},$$
$$\alpha_{\max_2}^{52} = 6\pi\sqrt{6}. \tag{33}$$

The potential between static sources in the fundamental and adjoint representations of the F_4 exceptional gauge group has been plotted in Fig. 6, along with the higher representations in the range $R \in [1, 100]$. The decomposition of the higher representations and the corresponding Cartan generators have been presented in Appendix A. In Fig. 6, screening is observed for the potentials of every representation at far distances. Since F_4 does not own any nontrivial center element, all representations act like $SU(N)$ representations with zero N-ality. Hence, screening was anticipated. Another reason for this phenomenon is the creation of gluons in the QCD vacuum that are able to screen the initial static color charges and produce a flat potential at high levels of energy:

$$52 \times 52 = \mathbf{1} \oplus 52 \oplus 324 \oplus \cdots,$$
$$273 \times 52 \times 52 \times 52 = \mathbf{1} \oplus 15(26) \oplus \cdots,$$
$$324 \times 52 \times 52 = \mathbf{1} \oplus 26 \oplus 3(52) \oplus \cdots. \tag{34}$$

Furthermore, in Fig. 6, there are linear parts at intermediate distance scales for all representations that are situated at the interval $R \in [2, 9]$, approximately. The linear potentials have been depicted in the lower diagram of Fig. 6. The slope of the linear potentials of different representations are given in the fourth column of Table II, as well as the potential ratios ($\frac{k_r}{k_F}$) in the last column. It is observed that potential ratios are qualitatively in agreement with Casimir scaling ($\frac{C_r}{C_F}$), which is presented in the third column of Table II. However, Casimir scaling has not been proved numerically for F_4.

Figure 7 presents the point-by-point ratio of the potential of each representation to the fundamental one in the range $R \in [1, 20]$. These ratios start up at the ratios of the corresponding Casimirs. However, they abruptly decline at intermediate intervals. The inclination becomes more pronounced as the dimension of the representations grows;

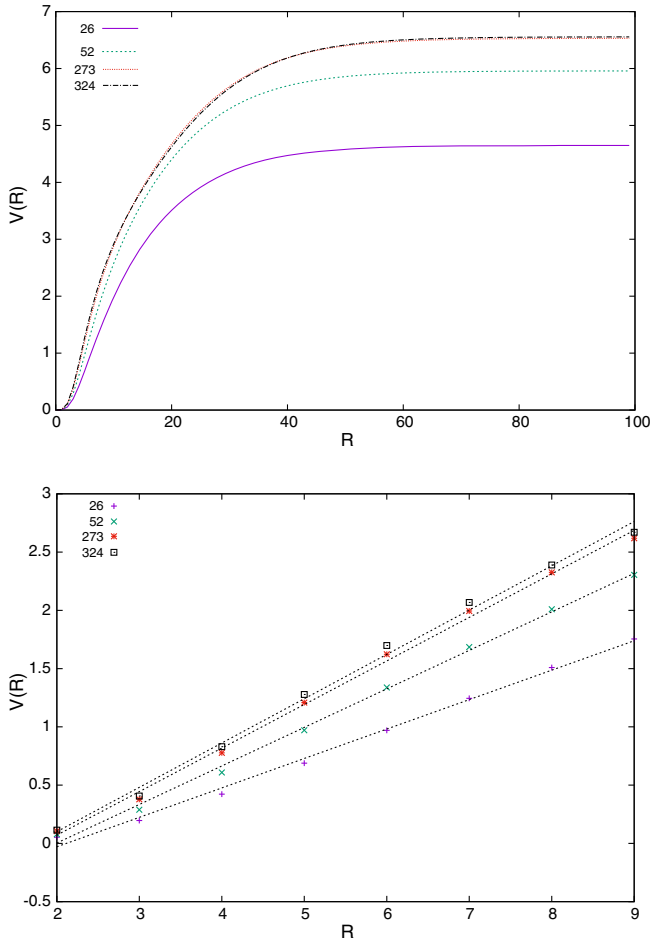

FIG. 6. Upper diagram: The potential between static color sources in the fundamental, adjoint, 273-dimensional, and 324-dimensional representations of the F_4 exceptional gauge group in the range $R \in [1, 100]$. All potentials are screened at far distances, while linearity is evident at intermediate parts. Lower diagram: The same as the upper diagram but in the range $R \in [2, 9]$. The slopes of the potentials have been given in the fourth row of Table II. The potentials are in agreement with Casimir scaling qualitatively.

TABLE II. Casimir numbers and Casimir ratios of different representations of the F_4 exceptional group are presented in the second and third columns, respectively [42].[a] The slopes of the linear potentials of Fig. 6 and the potential ratios are given in the fourth and fifth columns, respectively. The numbers in parentheses show the fit error.

Rep.	Casimir number	$\frac{C_r}{C_F}$	Potential slope	$\frac{k_r}{k_F}$
26	$\frac{2}{3}$	1	0.252(7)	1
52	1	1.5	0.331(7)	1.31(1)
273	2	2	0.374(8)	1.48(1)
324	$\frac{13}{9}$	2.16	0.38(1)	1.5(1)

[a]It should be noted that Casimir scaling of the representation 273 has not been reported in this reference.

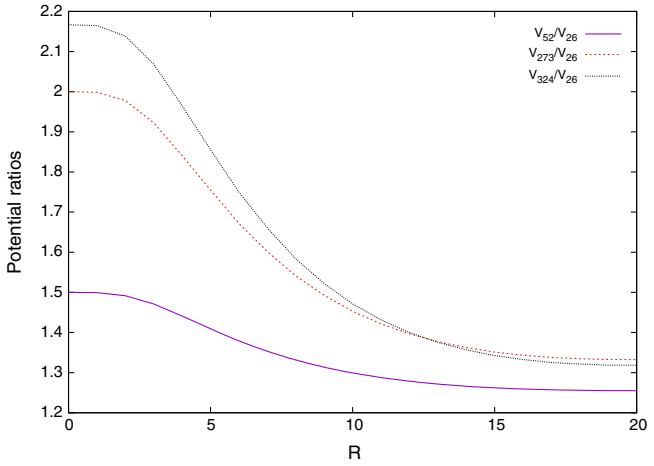

FIG. 7. Potential ratios of the F_4 representations to the fundamental one in the range $R \in [0, 20]$. These ratios start up at the values of the corresponding Casimir ratios presented in Table II.

e.g., the deviation from the exact Casimir scaling is more significant for representations 273 and 324.

To investigate whether the linear potentials of the F_4 exceptional group are caused by the nontrivial center elements of the $SU(3) \times SU(3)$ subgroup or not, one may plot the group factor function $\mathrm{Re}\mathcal{G}_r[\vec{\alpha}]$ with respect to the nontrivial center elements of $SU(3)$. Using the same method as in Refs. [28–30] and Eqs. (13) and (31), we are able to compose matrices containing center elements of $SU(3)$ depending on the N-ality of each representation. Thus,

$$\begin{aligned}
\mathbb{Z}^{26}_{SU(3)} &= \mathrm{diag}[1,1,1,1,1,1,1,1,z\mathbb{I}_{3\times3}, z\mathbb{I}_{3\times3}, z\mathbb{I}_{3\times3}, \\
&\quad z^*\mathbb{I}_{3\times3}, z^*\mathbb{I}_{3\times3}, z^*\mathbb{I}_{3\times3}], \\
\mathbb{Z}^{52}_{SU(3)} &= \mathrm{diag}[1,1,1,1,1,1,1,1,\mathbb{I}_{8\times8}, z\mathbb{I}_{3\times3}, z\mathbb{I}_{3\times3}, \\
&\quad z\mathbb{I}_{3\times3}, z\mathbb{I}_{3\times3}, z\mathbb{I}_{3\times3}, z\mathbb{I}_{3\times3}, z^*\mathbb{I}_{3\times3}, \\
&\quad z^*\mathbb{I}_{3\times3}, z^*\mathbb{I}_{3\times3}, z^*\mathbb{I}_{3\times3}, z^*\mathbb{I}_{3\times3}, z^*\mathbb{I}_{3\times3}],
\end{aligned} \tag{35}$$

where $z = \exp(\pm\frac{2\pi i}{3})$ is the $SU(3)$ nontrivial center element. We previously mentioned that z and z^* vortices carry the same magnetic fluxes but in the opposite directions. Interestingly, the numbers of z and z^* vortices that appear in the above decompositions of Eq. (35) are the same. Therefore, one might conclude that the F_4 vacuum domain consists of the $SU(3)$ center vortices. For our purpose, we use the normalization condition as follows:

$$\exp[i\vec{\alpha}\cdot\vec{H}^{26 \text{ or } 52}] = \mathbb{Z}^{26 \text{ or } 52}_{SU(3)}\mathbb{I}, \tag{36}$$

where H^{26} and H^{52} are the generators depicted in Eqs. (25) and (32), respectively. Solving the corresponding equations results in

$$\begin{aligned}
\alpha^{26-\mathrm{non}}_{\mathrm{max}_1} &= 2\pi\sqrt{6}, \\
\alpha^{26-\mathrm{non}}_{\mathrm{max}_2} &= 2\pi\sqrt{2},
\end{aligned} \tag{37}$$

and

$$\begin{aligned}
\alpha^{52-\mathrm{non}}_{\mathrm{max}_1} &= 6\pi\sqrt{2}, \\
\alpha^{52-\mathrm{non}}_{\mathrm{max}_2} &= 2\pi\sqrt{6},
\end{aligned} \tag{38}$$

where the term "non" denotes a nontrivial center element. It should be mentioned that an unusual normalization condition has been applied in Eq. (36). Therefore, neither the G_2 potentials nor the $SU(3)$ ones are expected. However, as the Cartan generators of Eq. (25) are taken, we expect the potentials obtained from Eqs. (37) and (38) to be parallel to the corresponding ones in Fig. 6, in some range of R. To study this fact more accurately, we study the group factor function.

The minimum points of the group factor function, which happen at the positions where half of the vortex flux enters the Wilson loop, are responsible for the intermediate linear potential. Therefore, we compare the group factors of different representations of F_4 obtained from the trivial center element with the ones calculated from the decomposition into the $SU(3)$ subgroup.

Figure 8 shows the real part of the group factor function for both fundamental and adjoint representations of the group F_4 and the $SU(3)$ subgroup using its nontrivial center elements. The discrepancies in the minimum amounts of the group factors in these figures are undeniable. As a result, one might say that the center elements of the $SU(3)$ subgroup are not the direct factors for the confinement of the F_4 static potentials. The same reason is applicable for the higher representations of the F_4 exceptional group. The calculations of the higher representations have been presented in Appendix A.

So far, we have shown that the decomposition of the F_4 representations into the $SU(3)$ subgroup leads to the Cartan generators that give the exact potential of F_4, and Casimir scaling is also achieved. However, the $SU(3)$ nontrivial center elements are not responsible for the linearity observed in the potentials of the F_4 representations. So, what accounts for the temporary confining potential? To answer this question, we study other subgroups of F_4. Greensite *et al.* [24] found that $SU(3)$ and Z_3-projected lattices are successful in reproducing the asymptotic string tension of G_2 gauge theory. However, no correlation between the gauge invariant Wilson loops and the $SU(3)$ and Z_3-projected loops is observed. They conclude that the results of the $SU(3)$ and Z_3 projections in G_2 gauge theory are misleading. Therefore, they look for the smallest subgroup of G_2, i.e., $SU(2)$, and the Wilson loop imposing a "maximal $SU(2)$" gauge is calculated. It is observed that the potential of the full G_2 theory is approximately parallel to the one obtained from the $SU(2)$-only Wilson loop. However, $SU(2)$ projection also appears to be problematic.

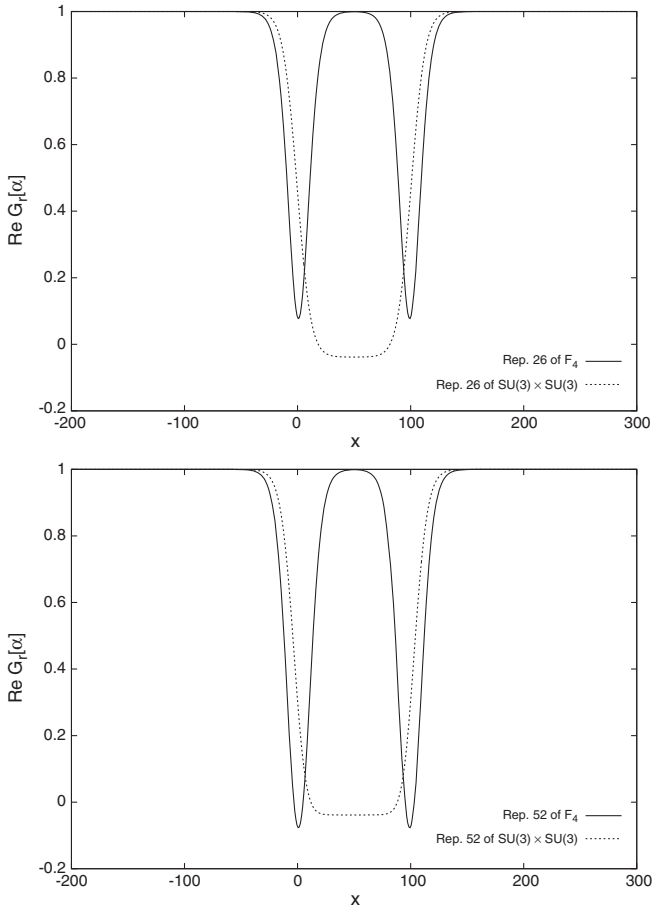

FIG. 8. The real part of the group factor versus the location x of the vacuum domain midpoint, for $R = 100$ and in the range $x \in [-200, 300]$, for the fundamental and adjoint representation of F_4 (solid lines) in comparison with the corresponding ones obtained from the $SU(3) \times SU(3)$ decomposition using its nontrivial center elements (dashed lines). The minimum values of the F_4 group factor for the fundamental and adjoint representations are 0.076 and -0.076, respectively. It is clear that the minimum value of the group factors for the $SU(3) \times SU(3)$ decomposition is not identical to the corresponding ones for F_4.

2. $SU(2) \times Sp(6)$ subgroup

We try to achieve pure $SU(N)$ subgroups of F_4 out of this decomposition. One may focus on the $Sp(6)$ to branch it out to its $SU(2)$ subgroups, using the following process:

$$Sp(6) \supset SU(2) \times Sp(4) \quad (R) \tag{39}$$

and then

$$Sp(4) \supset SU(2) \times SU(2) \quad (R). \tag{40}$$

Therefore, F_4 branches to a pure $SU(2)$ subgroup. For the fundamental and adjoint representations of F_4, one may have [36,37]

$$\begin{aligned} F_4 &\supset SU(2) \times Sp(6) \\ 26 &= (2,6) \oplus (1,14), \\ 52 &= (3,1) \oplus (1,21) \oplus (2,14'). \end{aligned} \tag{41}$$

In the next step,

$$\begin{aligned} Sp(6) &\supset SU(2) \times Sp(4) \\ 6 &= (2,1) \oplus (1,4), \\ 14 &= (1,1) \oplus (1,5) \oplus (2,4), \\ 14' &= (1,4) \oplus (2,5), \\ 21 &= (3,1) \oplus (1,10) \oplus (2,4). \end{aligned} \tag{42}$$

Then,

$$\begin{aligned} Sp(4) &\supset SU(2) \times SU(2) \\ 4 &= (2,1) \oplus (1,2), \\ 5 &= (1,1) \oplus (2,2), \\ 10 &= (3,1) \oplus (1,3) \oplus (2,2). \end{aligned} \tag{43}$$

Ultimately, for the F_4 exceptional group, pure $SU(2)$ subgroups are formed:

$$\begin{aligned} 26 = {} & (2,1) \oplus (2,1) \oplus (1,2) \oplus (2,1) \oplus (2,1) \oplus (1,2) \\ & \oplus (1,1) \oplus (1,1) \oplus (2,2) \oplus (2,1) \oplus (1,2) \\ & \oplus (2,1) \oplus (1,2), \\ 52 = {} & (3,1) \oplus (3,1) \oplus (3,1) \oplus (1,3) \oplus (2,2) \oplus (2,1) \\ & \oplus (1,2) \oplus (2,1) \oplus (1,2) \oplus (2,1) \oplus (1,2) \oplus (1,1) \\ & \oplus (2,2) \oplus (1,1) \oplus (2,2) \oplus (2,1) \oplus (1,2) \oplus (1,1) \\ & \oplus (2,2) \oplus (1,1) \oplus (2,2). \end{aligned} \tag{44}$$

The Cartan generators extracted out of these decompositions are

$$\begin{aligned} H^{26}_{SU(2)} = {} & \frac{1}{\sqrt{6}} \mathrm{diag}[0,0,0,0,\sigma_3^2,0,0,0,0,\sigma_3^2,0,0,\sigma_3^2,\sigma_3^2, \\ & 0,0,\sigma_3^2,0,0,\sigma_3^2], \\ H^{52}_{SU(2)} = {} & \frac{1}{3\sqrt{2}} \mathrm{diag}[0,0,0,0,0,0,0,0,0,\sigma_3^3,\sigma_3^2,\sigma_3^2,0,0, \\ & \sigma_3^2,0,0,\sigma_3^2,0,0,\sigma_3^2,0,\sigma_3^2,\sigma_3^2,0,\sigma_3^2,\sigma_3^2,0,0,\sigma_3^2, \\ & 0,\sigma_3^2,\sigma_3^2,0,\sigma_3^2,\sigma_3^2], \end{aligned} \tag{45}$$

where $\sigma_3^2 = \frac{1}{2}\mathrm{diag}[1,-1]$ and $\sigma_3^3 = \mathrm{diag}[1,0,-1]$ are diagonal generators of the $SU(2)$ gauge group in the fundamental and adjoint representations, respectively. Hence, with respect to the $SU(2)$ subgroup, we can reconstruct just one diagonal generator. It should be recalled that matrices of

Eq. (45) are normalized with the normalization condition in Eq. (17). Considering the normalization coefficient, it is obvious that the components of these matrices are identical to H_3^{26} and H_3^{52} in Eqs. (25) and (32), respectively. Therefore, one expects the potential between static color sources in the fundamental and adjoint representations to be the same as in Fig. 6, using the maximum flux values below:

$$\alpha_{\max}^{26} = 4\pi\sqrt{6},$$
$$\alpha_{\max}^{52} = 12\pi\sqrt{2}. \tag{46}$$

The next step is to investigate if the nontrivial center element of $SU(2)$, i.e., $z_1^{SU(2)} = e^{i\pi}$, is responsible for the confinement of F_4. So, we calculate the maximum flux values from Eq. (6).

Similar to what we did for the $SU(3)$ subgroup, we are going to develop matrices containing the nontrivial center element of the $SU(2)$ subgroup corresponding to the decomposition of Eq. (44):

$$\begin{aligned}\mathbb{Z}_{SU(2)}^{26} &= \mathrm{diag}[1,1,1,1,z_1\mathbb{I}_{2\times2},1,1,1,1,z_1\mathbb{I}_{2\times2},1,1,\\ &\quad z_1\mathbb{I}_{2\times2},z_1\mathbb{I}_{2\times2},1,1,z_1\mathbb{I}_{2\times2},1,1,z_1\mathbb{I}_{2\times2}],\\ \mathbb{Z}_{SU(2)}^{52} &= \mathrm{diag}[1,1,1,1,1,1,1,1,1,\mathbb{I}_{3\times3},z_1\mathbb{I}_{2\times2},z_1\mathbb{I}_{2\times2},\\ &\quad 1,1,z_1\mathbb{I}_{2\times2},1,1,z_1\mathbb{I}_{2\times2},1,1,z_1\mathbb{I}_{2\times2},1,z_1\mathbb{I}_{2\times2},\\ &\quad z_1\mathbb{I}_{2\times2},1,z_1\mathbb{I}_{2\times2},z_1\mathbb{I}_{2\times2},1,1,z_1\mathbb{I}_{2\times2},1,z_1\mathbb{I}_{2\times2},\\ &\quad z_1\mathbb{I}_{2\times2},1,z_1\mathbb{I}_{2\times2},z_1\mathbb{I}_{2\times2}],\end{aligned} \tag{47}$$

where $\mathbb{I}_{n\times n}$ are square identity matrices. Because the representations 2 and $\bar{2}$ are the same in $SU(2)$, the vortices z_1 and z_1^* are the same in this gauge group. It is observed that there are an even number of z_1 vortices in the decompositions of Eq. (47). Therefore, the vacuum domain or the trivial vortex might be thought to have these center vortices inside.

The maximum flux condition of Eq. (6) could be written as follows:

$$\exp[i\vec{\alpha}\cdot\vec{H}_{SU(2)}^{(26)\text{ or }(52)}] = \mathbb{Z}_{SU(2)}^{(26)\text{ or }(52)}\mathbb{I}, \tag{48}$$

which leads to the amounts

$$\alpha_{\max}^{26-\text{non}} = 2\pi\sqrt{6},$$
$$\alpha_{\max}^{52-\text{non}} = 6\pi\sqrt{2}. \tag{49}$$

To compare the extremums of the group factor function of the F_4 exceptional group with its $SU(2)$ subgroup, the real part of this function has been plotted versus the location of the vortex midpoint for the fundamental and adjoint representations in Fig. 9. It is observed that the group factors corresponding to this decomposition reach the amounts 0.076 and −0.076 at $x = 50$ for the fundamental and adjoint representations, respectively. These amounts are identical to the corresponding ones for F_4,

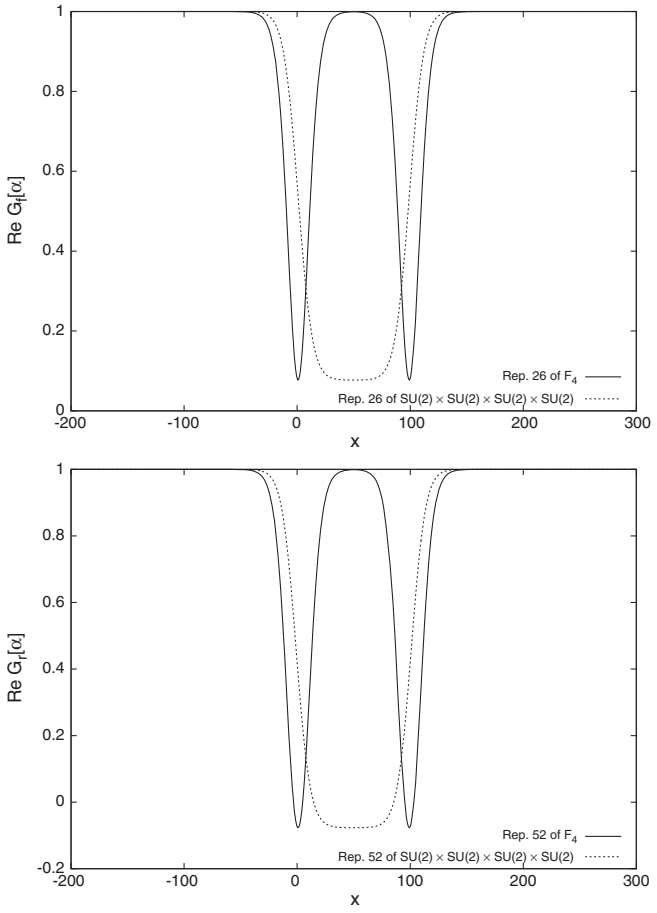

FIG. 9. The same as Fig. 8 but the dashed lines represent the group factor for the $SU(2)\times SP(6)\supset SU(2)\times SU(2)\times SP(4)\supset SU(2)\times SU(2)\times SU(2)\times SU(2)$ decomposition. In each diagram, the minimum values of the F_4 group factor are the same as the corresponding ones obtained from the $SU(2)$ subgroup. These values are 0.076 and −0.076 for the fundamental and adjoint representations, respectively.

which occur at $x = 0$ and $x = 100$. Since the extremums at $x = 50$ imply the complete interaction between vortices and the Wilson loop that results in a linear asymptotic potential, it is the center element of the $SU(2)$ subgroup that gives rise to the intermediate linear potential of F_4.

The other chain of possible decomposition is

$$F_4 \supset SU(2)\times Sp(6) \quad (R)$$
$$Sp(6) \supset SU(2)\times SU(2) \quad (S). \tag{50}$$

This decomposition generates matrices similar to h_3 and h_4. According to our previous discussion in Fig. 5, when h_3 or h_4 is applied, the minimum points of the group factor function are not identical to the ones for the F_4 gauge group. Using this fact, one might conclude that this decomposition is not responsible for the confinement in F_4.

3. $SO(9)$ subgroup

Another regular maximal subgroup of F_4 group is $SO(9)$. To extract a pure $SU(N)$ subgroup out of this subgroup, one might choose the following decomposition process:

$$SO(9) \supset SU(2) \times SU(4) \quad (R). \tag{51}$$

We present three methods to decompose $SU(4)$ into the $SU(2)$ subgroups:

(i) A regular decomposition as follows:

$$SU(4) \supset SU(2) \times SU(2) \times U(1). \tag{52}$$

There is a $U(1)$ factor in this decomposition that makes it a nonsemisimple maximal subgroup. In fact, the $U(1)$ that appears in some branching rules is a trivial Abelian Lie group composed by all 1×1 matrices of $e^{i\phi}$ with real ϕ [43]. This factor is excluded in the branching rules [36,44]. In our case, we ignore it since it has no effect on our calculations. If we evade the $U(1)$ factor in Eq. (52), the same results as in Eq. (44), where F_4 has been decomposed into its pure $SU(2)$ subgroups, are achieved. Hence, this decomposition could be responsible for the intermediate linear potentials, as well. As the results for the fundamental and adjoint representations are the same as in Fig. 9, we just present the detailed calculations for the higher representations in Appendix B.

(ii) $SU(4)$ has a singular subgroup,

$$SU(4) \supset Sp(4) \quad (S), \tag{53}$$

and it could be decomposed as follows:

$$Sp(4) \supset SU(2) \times SU(2) \quad (R). \tag{54}$$

The exact decompositions as in Eq. (44) and Cartan generators of Eq. (45) are obtained. Therefore, the same results are achieved. Consequently, singular maximal subgroups are able to bring out the same potentials as F_4 as well. Furthermore, this decomposition could also describe the linear potential of F_4 correctly.

(iii) Another chain of breaking to $SU(N)$ subgroups could be a singular decomposition:

$$SU(4) \supset SU(2) \times SU(2)(S). \tag{55}$$

Although this decomposition seems to be similar to Eq. (52), due to the branching rules, representations decompose in a way that they produce exact matrices as h_3 and h_4 of Eq. (14) in the fundamental representation of F_4. We previously learned that induced potentials by these matrices have different behaviors according to Fig. 5.

So far, we can conclude that, in order to determine the subgroups whose Cartan decompositions result in a well-defined potential, one has to compare reconstructed Cartan matrices produced by means of the subgroups with the ones of the main exceptional group itself. In the F_4 case, the potential out of applying all of its Cartan generators is the same as the case where just h_1 or h_2 is used. Therefore, any regular or singular subgroup that is able to reconstruct the same diagonal matrices as one of these two generators produces the same potential as that of F_4 itself.

4. $SU(2) \times G_2$ subgroup

Ultimately, we are going to investigate the results of a direct singular maximal subgroup of the F_4 exceptional group, i.e., $SU(2) \times G_2$, because it shows a different behavior. To make a pure $SU(N)$ subgroup out of this singular subgroup, one may choose to break G_2 into its $SU(3)$ subgroup:

$$G_2 \supset SU(3) \quad (R). \tag{56}$$

It is obviously not a pure subgroup because it contains both $SU(2)$ and $SU(3)$ subgroups. However, if one considers the representations of $SU(2)$ as degeneracies of the irreducible representations of $SU(3)$ in the branching rules, the result will be the same as the $F_4 \supset SU(3) \times SU(3)$ decomposition. We have argued that this decomposition is not responsible for the F_4 confinement.

A more challenging procedure is the following decomposition:

$$\begin{aligned} &F_4 \supset SU(2) \times G_2 \quad (S) \\ &26 = (5,1) \oplus (3,7), \\ &52 = (3,1) \oplus (1,14) \oplus (5,7). \end{aligned} \tag{57}$$

G_2 might be decomposed as

$$\begin{aligned} &G_2 \supset SU(2) \times SU(2) \quad (R) \\ &7 = (2,2) \oplus (1,3), \\ &14 = (3,1) \oplus (2,4) \oplus (1,3). \end{aligned} \tag{58}$$

Finally,

$$\begin{aligned} 26 = {} & (5,1) \oplus (2,2) \oplus (1,3) \oplus (2,2) \oplus (1,3) \\ & \oplus (2,2) \oplus (1,3) \\ 52 = {} & (3,1) \oplus (3,1) \oplus (2,4) \oplus (1,3) \oplus (2,2) \\ & \oplus (1,3) \oplus (2,2) \oplus (1,3) \oplus (2,2) \oplus (1,3) \\ & \oplus (2,2) \oplus (1,3) \oplus (2,2) \oplus (1,3). \end{aligned} \tag{59}$$

Using these decompositions, we can reproduce Cartan generators in the fundamental and adjoint representations as follows:

$$H^{26}_{SU(2)\times G_2} = \frac{1}{3\sqrt{2}}\mathrm{diag}[0,0,0,0,0,\sigma_3^2,\sigma_3^2,\sigma_3^3,\sigma_3^2,\sigma_3^2,\sigma_3^3,\sigma_3^2,\sigma_3^2,\sigma_3^3],$$
$$H^{52}_{SU(2)\times G_2} = \frac{1}{3\sqrt{6}}\mathrm{diag}[0,0,0,0,0,0,\sigma_3^4,\sigma_3^4,\sigma_3^3,\sigma_3^2,\sigma_3^2,\sigma_3^3,\sigma_3^2,\sigma_3^2,\sigma_3^3,\sigma_3^2,\sigma_3^2,\sigma_3^3,\sigma_3^2,\sigma_3^2,\sigma_3^3,\sigma_3^2,\sigma_3^2,\sigma_3^3]. \quad (60)$$

In these matrices, the normalization coefficients have been computed from Eq. (17). σ_3^2, σ_3^3, and σ_3^4 are Cartan generators of the $SU(2)$ gauge group in the fundamental, adjoint and four-dimensional representations, respectively. After an initial review, the elements of these matrices are not fully the same as the corresponding ones in Eqs. (25) and (32) or (45). Accordingly, the trivial static potentials, when we consider the trivial center element of the $SU(2)$ subgroup, are not identical to those of the F_4 exceptional group itself. We have investigated this subgroup in Ref. [45]. However, there is another aspect of this decomposition that is appealing.

The center element matrices of the $SU(2)\times G_2$ subgroup of F_4 in the fundamental and adjoint representations are given by

$$\mathbb{Z}^{26}_{SU(2)\times G_2} = \mathrm{diag}[1,1,1,1,1,z_1\mathbb{I}_{2\times2},z_1\mathbb{I}_{2\times2},\mathbb{I}_{3\times3},z_1\mathbb{I}_{2\times2},z_1\mathbb{I}_{2\times2},\mathbb{I}_{3\times3},z_1\mathbb{I}_{2\times2},z_1\mathbb{I}_{2\times2},\mathbb{I}_{3\times3}],$$
$$\mathbb{Z}^{52}_{SU(2)\times G_2} = \mathrm{diag}[1,1,1,1,1,1,z_1\mathbb{I}_{4\times4},z_1\mathbb{I}_{4\times4},\mathbb{I}_{3\times3},z_1\mathbb{I}_{2\times2},z_1\mathbb{I}_{2\times2},\mathbb{I}_{3\times3},z_1\mathbb{I}_{2\times2},z_1\mathbb{I}_{2\times2},\mathbb{I}_{3\times3},z_1\mathbb{I}_{2\times2},z_1\mathbb{I}_{2\times2},\mathbb{I}_{3\times3},z_1\mathbb{I}_{2\times2},z_1\mathbb{I}_{2\times2},\mathbb{I}_{3\times3}]. \quad (61)$$

Now, putting the above matrices in Eq. (6), the maximum flux values are calculated as follows:

$$\alpha_{\max}^{26\text{-non}} = 6\pi\sqrt{2},$$
$$\alpha_{\max}^{52\text{-non}} = 6\pi\sqrt{6}. \quad (62)$$

Figure 10 shows the group factor function versus the vortex midpoint x for the fundamental and adjoint representations, respectively. As observed, the group factor has a totally different behavior in comparison with Fig. 9. The minimum points of the F_4 representations occur at $x=0$ and $x=100$, where half of the vortex flux enters the Wilson loop. These points are responsible for the intermediate linear potentials of F_4. Now, we focus on the

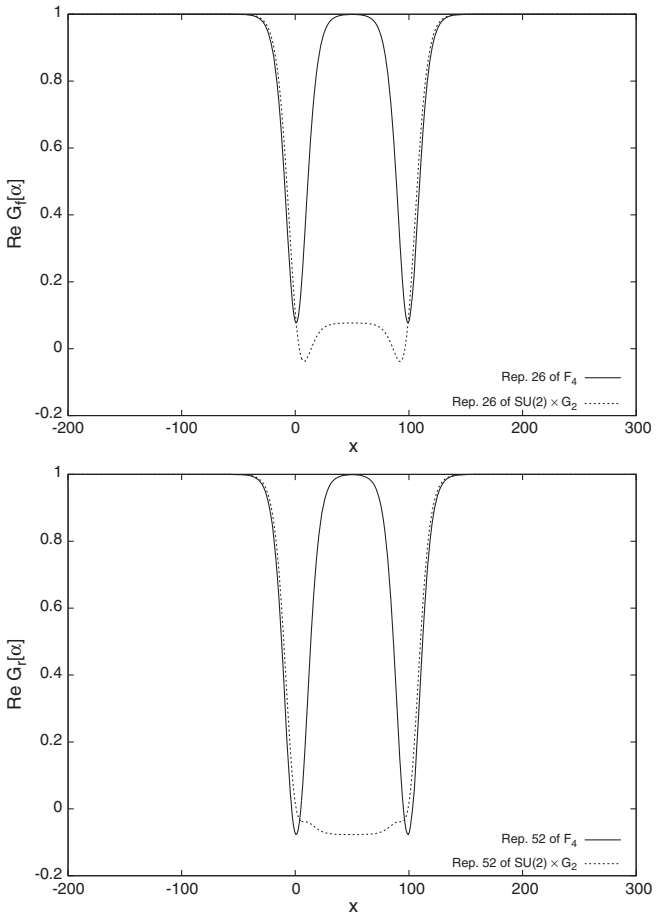

FIG. 10. The same as Fig. 9 but for the $SU(2)\times G_2$ subgroup. In both figures, the minimum values of the F_4 group factor are identical to the amount of the group factor corresponding to the $SU(2)\times G_2$ decomposition at $x=50$. Therefore, the slope of the intermediate linear of F_4 is the same as the asymptotic one for the $SU(2)\times G_2$ subgroup.

decomposition of the representations to the $SU(2)\times G_2$ subgroup. When the vortex midpoint is located at $x=50$, it means that the vortex is completely inside the Wilson loop. The nonzero value of the group factor at this point results in a linear potential at large distances. As the value of the group factor at this point is equal to the corresponding one for F_4, the slope of this linear potential seems to be identical to the intermediate linear potentials of F_4. Therefore, one might say that the $SU(2)\times G_2 \supset SU(2)\times SU(2)\times SU(2)$ subgroup of F_4 is responsible for the intermediate confinement of this exceptional group.

An interesting point here is that Cartan generators of this decomposition are different from h_1 and h_2. However, the minimum points of the F_4 group factor can still be investigated correctly via this decomposition. The question is why this happens. In fact, the N-ality of the $SU(N)$ representations or the center element matrix obtained from the group decompositions has the predominant responsibility here. The representations could be classified by their

N-ality. This means that the Wilson loop of the representations with the same N-ality is affected by a vortex type n in the same manner. To make it more clear, we investigate center element matrices of the fundamental representation in Eq. (47), obtained from the $SU(2)\times Sp(6)$ subgroup, and also in Eq. (61), by means of the $SU(2)\times G_2$ subgroup, which have different elements. In the former one, there exist fourteen 1's and six $z_1\mathbb{I}_{2\times2}$'s, while in the latter one, in Eq. (61), there exist five 1's, six $z_1\mathbb{I}_{2\times2}$'s, and three $\mathbb{I}_{3\times3}$'s. The number of $z_1\mathbb{I}_{2\times2}$ center elements is the same in both matrices, which corresponds to the fundamental representation with 2-ality $=1$. Elements 1 and $\mathbb{I}_{3\times3}$ with zero 2-ality have no effect on the Wilson loop. So, the other elements of these two matrices do not affect the Wilson loop. As a result, although the matrices of Eqs. (45) and (60) have different elements and the potentials of these two generators behave differently, the number of center vortices that emerge in both decompositions is the same. Thus, the group factor reaches the same minimum amount in both of them. Regarding 52-dimensional adjoint representation, the same process comes about.

B. E_6 exceptional group

E_6 is the third exceptional group in terms of largeness. It makes a 78-dimensional space with 78 generators and, similar to $SU(3)$, has $\mathbb{Z}_3$ as its group center [27]. Here, we mostly focus on its trivial center to investigate the static potential behavior. As the rank of E_6 is six, it possesses six diagonal matrices that are shown as follows for the fundamental representation [46]:

$$\begin{aligned}
h_1^{27} &= N_1\mathrm{diag}[-1,+1,0,0,0,0,0,0,0,-1,0,0,0,-1,\\
&\quad +1,-1,-1,+1,+1,+1,0,-1,+1,0,0,0,0],\\
h_2^{27} &= N_2\mathrm{diag}[0,-1,+1,0,0,0,0,0,-1,+1,0,-1,-1,\\
&\quad +1,0,+1,0,0,0,-1,+1,0,-1,+1,0,0,0],\\
h_3^{27} &= N_3\mathrm{diag}[0,0,-1,+1,0,0,0,-1,+1,0,-1,+1,0,0,\\
&\quad 0,-1,+1,0,-1,+1,0,0,0,-1,+1,0,0],\\
h_4^{27} &= N_4\mathrm{diag}[0,0,0,-1,+1,0,-1,+1,0,0,0,-1,+1,\\
&\quad -1,0,+1,0,-1,+1,0,0,0,0,0,-1,+1,0],\\
h_5^{27} &= N_5\mathrm{diag}[0,0,0,0,-1,+1,0,-1,-1,-1,+1,+1,0,\\
&\quad +1,-1,0,0,+1,0,0,0,0,0,0,0,-1,+1],\\
h_6^{27} &= N_6\mathrm{diag}[0,0,0,-1,-1,-1,+1,+1,0,0,+1,0,0,0,\\
&\quad 0,0,-1,0,0,-1,-1,+1,+1,+1,0,0,0].
\end{aligned} \tag{63}$$

These matrices are normalized and their normalization coefficients could be calculated from Eq. (17):

$$N_1=\cdots=N_6=\frac{1}{2\sqrt{6}}. \tag{64}$$

It should be noted that, due to the similarity of these matrices, one can use only h_1^{27} to calculate the potential of the fundamental representation of E_6. The maximum flux values for the domain structures, calculated from the condition in Eq. (19), are

$$\alpha_1^{\max}=\cdots=\alpha_6^{\max}=2\pi\sqrt{24}. \tag{65}$$

On the other hand, if we include the nontrivial flux condition in Eq. (6), the maximum amounts for the vortex fluxes are

$$\begin{aligned}
\alpha_{\max_1}^{\mathrm{non}}=\alpha_{\max_4}^{\mathrm{non}} &= \mp\frac{4\pi}{3}\sqrt{6},\\
\alpha_{\max_3}^{\mathrm{non}}=\alpha_{\max_6}^{\mathrm{non}} &= \mp 4\pi\sqrt{6},\\
\alpha_{\max_2}^{\mathrm{non}}=\alpha_{\max_5}^{\mathrm{non}} &= \mp\frac{8\pi}{3}\sqrt{6},
\end{aligned} \tag{66}$$

where "non" indicates the answer pertaining to the nontrivial center elements. Negative answers have been gained by type 1 vortices when Eq. (6) is equal to $z_1=\exp(\frac{2\pi i}{3})$ and positive answers correspond to the type 2 vortices $[z_2=\exp(\frac{-2\pi i}{3})]$. Static potentials obtained by both of these maximum trivial and nontrivial flux values in Eqs. (65) and (66) have been depicted in Fig. 11. As could have been predicted, at far distances, the potential obtained from the trivial center element of E_6 has been screened while the potential corresponding to the nontrivial center element is linear. This fact could be investigated by tensor products of the E_6 "quark" and "gluons":

$$27\times78=27\oplus351\oplus1728. \tag{67}$$

It is seen that E_6 "gluons" are not able to screen the potential of the E_6 "quarks". Similar to $SU(N)$ gauge

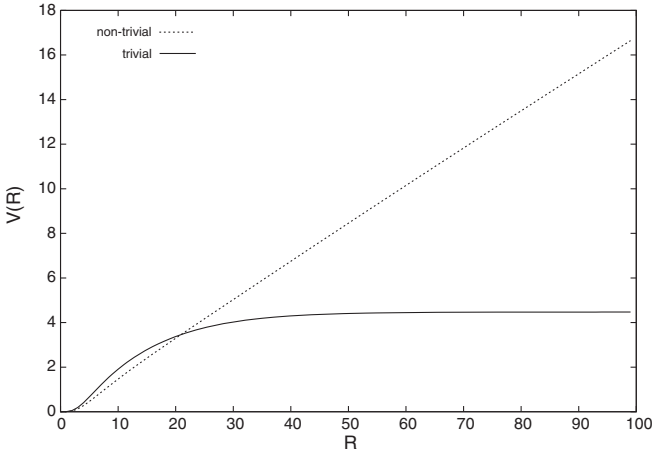

FIG. 11. Potential of the fundamental representation of E_6 using trivial and nontrivial center elements for $R\in[1,100]$.

groups, one "quark" and one "antiquark" can join to create a meson,

$$27 \times \overline{27} = 1 \oplus 78 \oplus 650, \tag{68}$$

and three "quarks" form a baryon,

$$27 \times 27 \times 27 = 1 \oplus 2(78) \oplus 3(650) \oplus 2925 \oplus \overline{3003} \oplus 2\overline{5824}. \tag{69}$$

Now, we aim to follow the same procedure applied for F_4 to explain what actually accounts for the temporary confinement in the trivial static potential of the E_6 exceptional group. The main question is, which kinds of center vortices have filled the E_6 QCD vacuum that give rise to the intermediate confining potential obtained by the trivial center element? In general, we have three candidates:

(i) Nontrivial center elements of the E_6 exceptional group;
(ii) Nontrivial center elements of its $SU(3)$ maximal subgroup;
(iii) Nontrivial center elements of its maximal $SU(2)$ subgroup.

To answer this question properly, the group factor function using Eq. (63) for both trivial and nontrivial center elements of the E_6 exceptional group have been demonstrated in Fig. 12. Consequently, nontrivial center elements of E_6 are not the direct reason of the intermediate linear part in the trivial potential of E_6. Then, we go for some of the maximal subgroups of E_6 that have been mentioned in Table I.

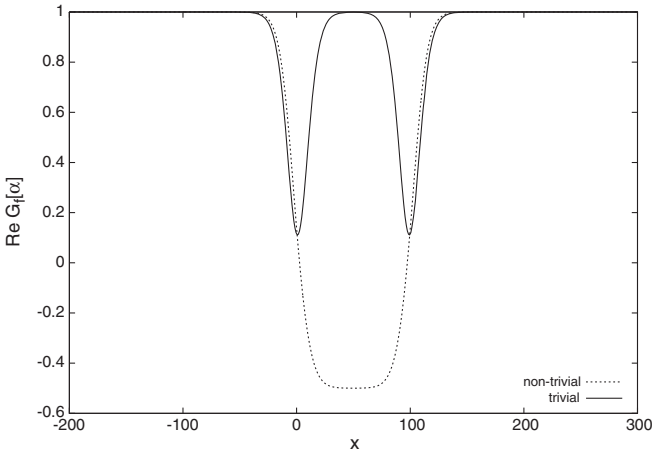

FIG. 12. Solid line represents the group factor of the fundamental representation of E_6 versus the location x of the vacuum domain midpoint, using the trivial center element, for $R = 100$ in the range $x \in [-200, 300]$. The dashed line shows the same function versus the location x of the nontrivial center vortex.

1. $SU(3) \times SU(3) \times SU(3)$ subgroup

The fundamental representation decomposes as [36–38]

$$27 = (3, \bar{3}, 1) \oplus (1, 3, 3) \oplus (\bar{3}, 1, \bar{3}). \tag{70}$$

Thus, if we assume the first two representations in the parentheses in Eq. (70), as degeneracies step by step, one might have

$$27 = 9(1) \oplus 3(3) \oplus 3(\bar{3}). \tag{71}$$

Although E_6 has a nontrivial center element, the method of decomposing its representations leads to the $SU(3)$ representations with different trialities. Therefore, an E_6 "quark" could be decomposed into three $SU(3)$ quarks, three antiquarks, and nine singlets. Now, two Cartan generators with regard to this subgroup are reconstructed from Eq. (71):

$$H_a^{27} = \frac{1}{\sqrt{6}}\mathrm{diag}[0,0,0,0,0,0,0,0,0,\lambda_a^3,\lambda_a^3,\lambda_a^3, -(\lambda_a^3)^*, -(\lambda_a^3)^*, -(\lambda_a^3)^*], \tag{72}$$

where $a = 3, 8$. Now, one can consider the condition in Eq. (19) and find

$$\alpha_{\max_1}^{27} = 2\pi\sqrt{6}, \quad \alpha_{\max_2}^{27} = 6\pi\sqrt{2}. \tag{73}$$

The potential between the fundamental sources of the E_6 using the six Cartan generators in Eq. (63) has been presented in Fig. 13, which overlaps completely with the data obtained from the above values in Eq. (73) and Cartan generators of Eq. (72). This fact is the result of the identical

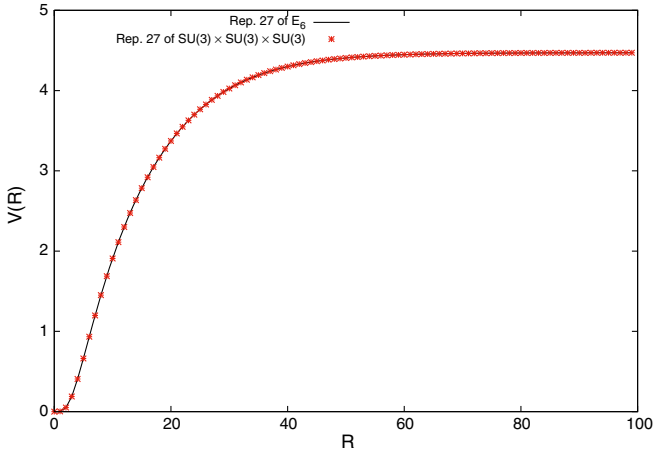

FIG. 13. The potential of the fundamental representation of E_6 using all Cartan generators (solid line) and the one corresponding to the $SU(3) \times SU(3) \times SU(3)$ decomposition (stars) in the range $R \in [1, 100]$. The two sets of data are the same.

components of H_3^{27} and h_1^{27}. Although H_8^{27} has different matrix elements, it has the same effect as H_3^{27} on the E_6 potentials. A similar discussion has been given in the $F_4 \supset SU(3) \times SU(3)$ decomposition. Therefore, one might use the $SU(3)$ subgroup decomposition to find the E_6 adjoint potential.

Reconstruction of Cartan generators in the adjoint representation of E_6 with respect to its $SU(3)$ subgroup is possible only when we want to calculate the trivial static potential because they are identical. This method is not applicable for the potentials obtained by the nontrivial center elements.

The adjoint representation might be decomposed as follows:

$$78 = (8,1,1) \oplus (1,8,1) \oplus (1,1,8) \oplus (3,3,\bar{3}) \oplus (\bar{3},\bar{3},3) = 16(1) \oplus 8 \oplus 9(\bar{3}) \oplus 9(3). \tag{74}$$

So, an E_6 "gluon" has been decomposed into nine $SU(3)$ quarks, nine antiquarks, one gluon, and 16 singlets. Hence, the Cartan generators structured from the $SU(3)$ decomposition are

$$H_a^{78} = \frac{1}{2\sqrt{6}}\mathrm{diag}[\overbrace{0,\ldots,0}^{8\text{ times}},\overbrace{0,\ldots,0}^{8\text{ times}},\lambda_a^8, \overbrace{-(\lambda_a^3)^*,\ldots,-(\lambda_a^3)^*}^{9\text{ times}},\overbrace{\lambda_a^3,\ldots,\lambda_a^3}^{9\text{ times}}]. \tag{75}$$

Applying the maximum flux condition of Eq. (19) for these Cartan generators, we have

$$\alpha_{\max_1}^{78} = 4\pi\sqrt{6}, \qquad \alpha_{\max_2}^{78} = 12\pi\sqrt{2}. \tag{76}$$

The potential between static color sources using the trivial center element of the E_6 exceptional gauge group for the fundamental and adjoint representations has been plotted in Fig. 14. The screening is visible at large distances, while the intermediate parts are linear. The lower diagram shows the linear parts of the potentials in the interval $R \in [3,10]$. We have fitted our data to the equation $V(R) = aR + b$. The slopes of the potentials have been found to be 0.251(3) and 0.309(5) for the fundamental and adjoint representations, respectively. Therefore, the ratio of the adjoint potential to the fundamental one in this range is 1.23(5). In fact, the ratio of the adjoint potential to the fundamental one starts from 1.384, which is the Casimir scaling of the adjoint representation [42]. But, similar to Fig. 7, the adjoint potential ratio differs from the exact value of Casimir scaling at intermediate distances.

To find what accounts for the intermediate linear potential, one needs to construct a matrix that consists of $SU(3)$ center elements with respect to Eqs. (70) and (74):

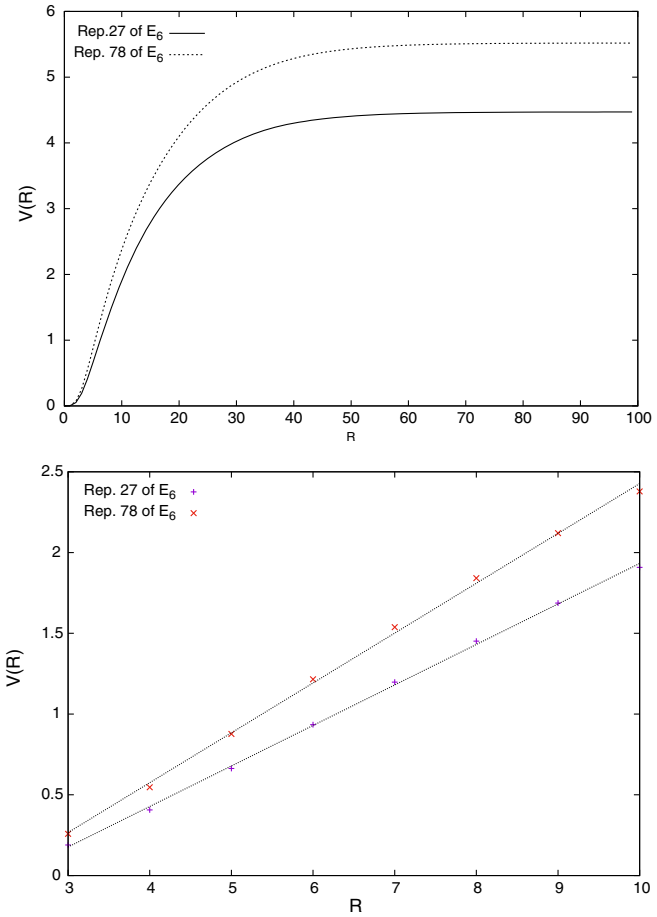

FIG. 14. Upper diagram: Trivial static potentials of the E_6 exceptional group for the fundamental and adjoint representations in the range $R \in [1,100]$. The potentials are screened at large distances, which is due to the absence of the nontrivial center element. At intermediate quark separations, the potentials are linear and have been presented in the lower diagram in the range $R \in [3,10]$. The ratio of the adjoint potential to the fundamental one is in agreement with Casimir scaling.

$$\mathbb{Z}_{SU(3)}^{27} = \mathrm{diag}[1,1,1,1,1,1,1,1,1,z\mathbb{I}_{3\times3},z\mathbb{I}_{3\times3}, z\mathbb{I}_{3\times3},z^*\mathbb{I}_{3\times3},z^*\mathbb{I}_{3\times3},z^*\mathbb{I}_{3\times3}],$$
$$\mathbb{Z}_{SU(3)}^{78} = \mathrm{diag}[\overbrace{0,\ldots,0}^{8\text{ times}},\overbrace{0,\ldots,0}^{8\text{ times}},\mathbb{I}_{8\times8}, \overbrace{z^*\mathbb{I}_{3\times3},\ldots,z^*\mathbb{I}_{3\times3}}^{9\text{ times}},\overbrace{z\mathbb{I}_{3\times3},\ldots,z\mathbb{I}_{3\times3}}^{9\text{ times}}]. \tag{77}$$

Similar to F_4, the numbers of z and z^* vortices are the same in the above matrices. Using Eq. (6), we have

$$\alpha_{\max_1}^{27\text{-non}} = 2\pi\sqrt{6}, \qquad \alpha_{\max_2}^{27\text{-non}} = 2\pi\sqrt{2},$$
$$\alpha_{\max_1}^{78\text{-non}} = 4\pi\sqrt{6}, \qquad \alpha_{\max_1}^{78\text{-non}} = 4\pi\sqrt{2}. \tag{78}$$

Using the above amounts, one might plot the group factor for the fundamental and adjoint representations in

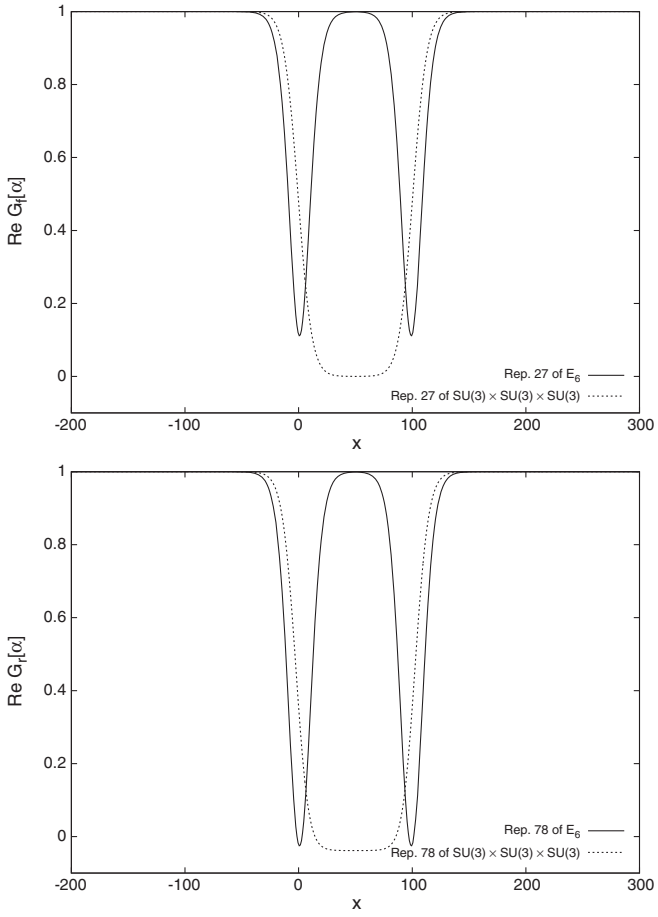

FIG. 15. The real part of the group factor function versus the location x of the vacuum domain midpoint, for $R = 100$ and in the range $x \in [-200, 300]$, for the fundamental and adjoint representation of E_6 (solid lines) in comparison with the same function versus the location x of the vortex midpoint obtained from the $SU(3) \times SU(3) \times SU(3)$ decomposition (dashed lines). The minimum points of the E_6 group factor that occur at $x = 0$ and $x = 100$ reach the amounts 0.111 and -0.025 for the fundamental and adjoint representations, respectively, whereas these amounts are approximately 0 and -0.038 for the $SU(3)$ subgroup.

Fig. 15 and compare them with the corresponding ones for E_6. In this figure, we can observe that the minimum values are not the same. Thus, nontrivial center elements of the $SU(3)$ subgroup are not in charge of the confining part in the trivial potential of E_6. The third possibility to investigate the linearity of the E_6 trivial potentials in Fig. 14 is the nontrivial center element of the $SU(2)$ subgroups.

2. $SU(2) \times SU(6)$ subgroup

Now, we decompose E_6 into the $SU(2) \times SU(6)$ subgroup and have

$$\begin{aligned} 27 &= (2, \bar{6}) \oplus (1, 15), \\ 78 &= (3, 1) \oplus (1, 35) \oplus (2, 20). \end{aligned} \tag{79}$$

Then, one can choose the following maximal subgroup of $SU(6)$ to decompose its representations:

$$\begin{aligned} &SU(6) \supset SU(2) \times SU(4) \times U(1) \quad (R) \\ &\quad 6 = (2,1) \oplus (1,4), \\ &\quad 15 = (1,1) \oplus (2,4) \oplus (1,6), \\ &\quad 20 = (1,4) \oplus (1,\bar{4}) \oplus (2,6), \\ &\quad 35 = (1,1) \oplus (3,1) \oplus (1,15) \oplus (2,4) \oplus (2,\bar{4}), \end{aligned} \tag{80}$$

and for $SU(4)$,

$$\begin{aligned} &SU(4) \supset SU(2) \times SU(2) \times U(1) \quad (R) \\ &\quad 4 = (2,1) \oplus (1,2), \\ &\quad 6 = (1,1) \oplus (1,1) \oplus (2,2), \\ &\quad 15 = (1,1) \oplus (3,1) \oplus (1,3) \oplus (2,2) \oplus (2,2). \end{aligned} \tag{81}$$

Finally, we have

$$\begin{aligned} 27 = {} & (2,1) \oplus (2,1) \oplus (1,2) \oplus (2,1) \oplus (2,1) \oplus (1,2) \\ & \oplus (1,1) \oplus (2,1) \oplus (1,2) \oplus (2,1) \oplus (1,2) \oplus (1,1) \\ & \oplus (1,1) \oplus (2,2), \\ 78 = {} & (3,1) \oplus (1,1) \oplus (3,1) \oplus (1,1) \oplus (3,1) \oplus (1,3) \\ & \oplus (2,2) \oplus (2,2) \oplus (2,1) \oplus (1,2) \oplus (2,1) \oplus (1,2) \\ & \oplus (2,1) \oplus (1,2) \oplus (2,1) \oplus (1,2) \oplus (2,1) \oplus (1,2) \\ & \oplus (2,1) \oplus (1,2) \oplus (1,1) \oplus (1,1) \oplus (2,2) \oplus (1,1) \\ & \oplus (1,1) \oplus (2,2) \oplus (2,1) \oplus (1,2) \oplus (2,1) \oplus (1,2) \\ & \oplus (1,1) \oplus (1,1) \oplus (2,2) \oplus (1,1) \oplus (1,1) \oplus (2,2). \end{aligned} \tag{82}$$

In Eqs. (80)–(82), the $U(1)$ factor has been ignored. Reconstruction of the Cartan generators for the $SU(2)$ subgroup of E_6 and for the fundamental and adjoint representations using the decompositions in Eq. (82) is as follows:

$$\begin{aligned} H^{27}_{SU(2)} = {} & \frac{1}{\sqrt{6}} \mathrm{diag}[0,0,0,0,\sigma_3^2,0,0,0,0,\sigma_3^2,0,0,0,\sigma_3^2, \\ & 0,0,\sigma_3^2,0,0,\sigma_3^2,\sigma_3^2], \\ H^{78}_{SU(2)} = {} & \frac{1}{2\sqrt{6}} \mathrm{diag}[\overbrace{0,\ldots,0}^{35\text{ times}},\sigma_3^3,\overbrace{\sigma_3^2,\ldots,\sigma_3^2}^{20\text{ times}}]. \end{aligned} \tag{83}$$

It should be noted that, for the sake of simplicity, the components of the matrix $H^{78}_{SU(2)}$ are not in order because it does not have any effect on our calculations.

To make a comparison with the potentials obtained from the trivial center element of the E_6 exceptional group and

its $SU(2)$ subgroup, one can utilize Eq. (83) in Eq. (19) and find

$$\alpha_{\max}^{27} = 4\pi\sqrt{6},$$
$$\alpha_{\max}^{78} = 8\pi\sqrt{6}. \tag{84}$$

Static potentials obtained by these maximum flux values and Cartans of Eq. (83) are identical to the E_6 potentials in Fig. 14. These results were foreseeable due to the similarity of the matrix components of Eq. (83) with the corresponding Cartan generators of E_6 in Eqs. (72) and (75).

Matrices made of center elements of the $SU(2)$ subgroup considering Eq. (82) are

$$\mathbb{Z}_{SU(2)}^{27} = [1,1,1,1,z_1\mathbb{I}_{2\times2},1,1,1,1,z_1,\mathbb{I}_{2\times2},1,1,1,$$
$$z_1\mathbb{I}_{2\times2},1,1,z_1\mathbb{I}_{2\times2},1,1,z_1\mathbb{I}_{2\times2},z_1\mathbb{I}_{2\times2}],$$
$$\mathbb{Z}_{SU(2)}^{78} = [\overbrace{1,\ldots,1}^{35\text{ times}},\mathbb{I}_{3\times3},\overbrace{z_1\mathbb{I}_{2\times2},\ldots,z_1\mathbb{I}_{2\times2}}^{20\text{ times}}]. \tag{85}$$

So, using Eq. (6), the flux maximum values are

$$\alpha_{\max}^{27\text{-non}} = 2\pi\sqrt{6},$$
$$\alpha_{\max}^{78\text{-non}} = 4\pi\sqrt{6}. \tag{86}$$

Using these values, we are able to plot the group factor function for the nontrivial center element of the $SU(2)$ subgroup and compare the results with the same function obtained by the trivial center element of the E_6 exceptional group or its $SU(3)$ subgroup. Figure 16 depicts this comparison. It is clear that the minimum points are identical. So, one can conclude that the nontrivial center element of the $SU(2)$ subgroup is responsible for the linearity at intermediate distance scales.

3. F_4 subgroup

There is another way to decompose E_6 into its subgroup without having a $U(1)$ factor in the final result. For instance, the decomposition chain described below can satisfy our assumption and reconstruct matrices with the same components as in Eq. (83):

$$E_6 \supset F_4 \quad (S)$$
$$F_4 \supset SU(2)\times Sp(6) \quad (R)$$
$$Sp(6) \supset SU(2)\times Sp(4) \quad (R)$$
$$Sp(4) \supset SU(2)\times SU(2) \quad (R). \tag{87}$$

Therefore, we expect the same result as the $E_6 \supset SU(2)\times SU(6)$ decomposition.

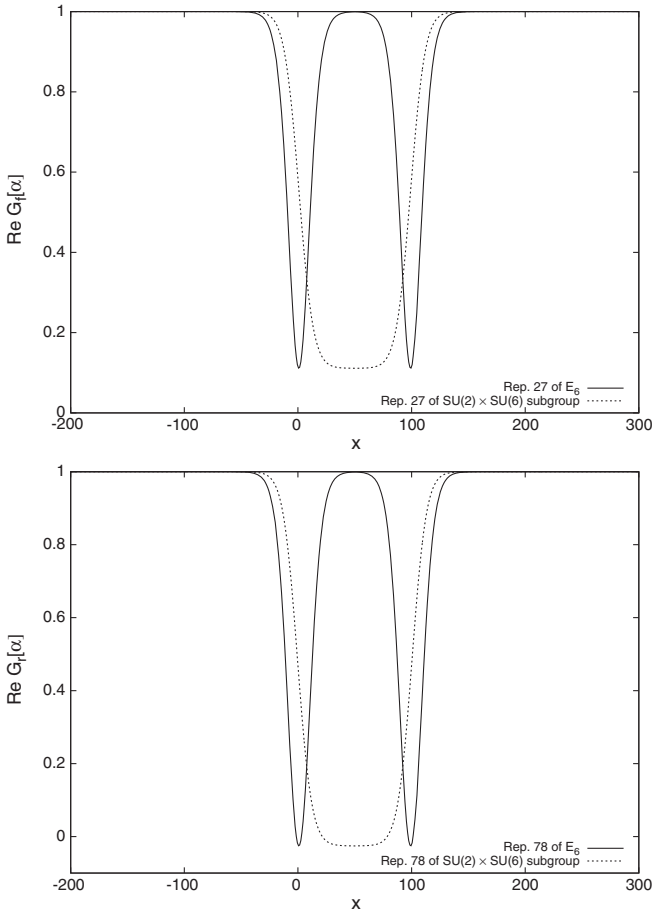

FIG. 16. The same as Fig. 15 but the dashed lines represent the group factor corresponding to the $SU(2)\times SU(6)$ subgroup of E_6. It is clear that in both diagrams, the minimum values are identical.

4. G_2 subgroup

In the F_4 exceptional group case, its singular maximal $SU(2)\times G_2$ subgroup has a property that could not produce the same potential as F_4 itself, because its reconstructed Cartan matrices consist of different components from h_1 and h_2 original Cartan generators of F_4. However, they are still able to produce the same linear part as some of the other $SU(2)$ subgroups of F_4. Here, for E_6, the branching G_2 singular maximal subgroup into the $SU(2)\times SU(2)$ subgroup attributes similarly to the $SU(2)\times G_2$ subgroup of F_4. According to the branching rules, the decomposition for the fundamental representation of the E_6 is as follows:

$$E_6 \supset G_2 \quad (S)$$
$$27 = 27$$
$$78 = 14 \oplus 64. \tag{88}$$

Then,

$$
\begin{aligned}
&G_2 \supset SU(2) \times SU(2) \quad (R)\\
&27 = (3,3) \oplus (2,4) \oplus (2,2) \oplus (1,5) \oplus (1,1),\\
&14 = (1,3) \oplus (2,4) \oplus (3,1),\\
&64 = (4,2) \oplus (3,5) \oplus (3,3) \oplus (2,6) \oplus (2,4) \oplus (2,2)\\
&\qquad \oplus (1,5) \oplus (1,3).
\end{aligned} \tag{89}
$$

Therefore,

$$
\begin{aligned}
H^{27}_{E_6 \supset G_2} &= \frac{1}{3\sqrt{6}}\mathrm{diag}[\sigma_3^3, \sigma_3^3, \sigma_3^3, \sigma_3^4, \sigma_3^4, \sigma_3^2, \sigma_3^2, \sigma_3^5, 0],\\
H^{78}_{E_6 \supset G_2} &= \frac{1}{6\sqrt{6}}\mathrm{diag}[\sigma_3^3, \sigma_3^4, \sigma_3^4, 0, 0, 0, \sigma_3^2, \sigma_3^2, \sigma_3^2, \sigma_3^2, \sigma_3^5,\\
&\quad \sigma_3^5, \sigma_3^5, \sigma_3^3, \sigma_3^3, \sigma_3^3, \sigma_3^6, \sigma_3^6, \sigma_3^4, \sigma_3^4, \sigma_3^2, \sigma_3^2, \sigma_3^5, \sigma_3^3],
\end{aligned} \tag{90}
$$

and

$$
\begin{aligned}
\mathbb{Z}^{27}_{E_6 \supset G_2} &= \mathrm{diag}[\mathbb{I}_{3\times3}, \mathbb{I}_{3\times3}, \mathbb{I}_{3\times3}, z_1\mathbb{I}_{4\times4}, z_1\mathbb{I}_{4\times4},\\
&\quad z_1\mathbb{I}_{2\times2}, z_1\mathbb{I}_{2\times2}, \mathbb{I}_{5\times5}, 1],\\
\mathbb{Z}^{78}_{E_6 \supset G_2} &= \mathrm{diag}[\mathbb{I}_{3\times3}, z_1\mathbb{I}_{4\times4}, z_1\mathbb{I}_{4\times4}, 1, 1, 1,\\
&\quad z_1\mathbb{I}_{2\times2}, z_1\mathbb{I}_{2\times2}, z_1\mathbb{I}_{2\times2}, z_1\mathbb{I}_{2\times2},\\
&\quad \mathbb{I}_{5\times5}, \mathbb{I}_{5\times5}, \mathbb{I}_{5\times5}, \mathbb{I}_{3\times3}, \mathbb{I}_{3\times3}, \mathbb{I}_{3\times3},\\
&\quad z_1\mathbb{I}_{6\times6}, z_1\mathbb{I}_{6\times6}, z_1\mathbb{I}_{4\times4}, z_1\mathbb{I}_{4\times4},\\
&\quad z_1\mathbb{I}_{2\times2}, z_1\mathbb{I}_{2\times2}, \mathbb{I}_{5\times5}, \mathbb{I}_{3\times3}],
\end{aligned} \tag{91}
$$

The flux condition of Eq. (19) gives

$$
\begin{aligned}
\alpha^{27\text{-non}}_{\max} &= 6\pi\sqrt{6},\\
\alpha^{78\text{-non}}_{SU(2)\text{-}\max} &= 12\pi\sqrt{6}.
\end{aligned} \tag{92}
$$

Figure 17 shows the group factor obtained from this decomposition versus the location x of the vortex midpoint. It is observed that the amount of the group factor when the vortex is completely inside the Wilson loop is equal to the minimum values of the E_6 group factor. Therefore, this decomposition is able to describe E_6 temporary confinement. It should be pointed out that the numbers of center elements that emerge in the center element matrices of Eqs. (85) and (90) are the same. So, an argument similar to that of the $SU(2) \times G_2$ subgroup of F_4 could be applied here.

C. G_2 exceptional group

G_2 is the simplest exceptional group with rank 2 and likewise $SU(3)$. All of its representations are real and it is its own universal covering group. Despite F_4 and E_6 exceptional groups that do not have numerical supports yet, pending future investigations, there are lattice calculations in favor of the G_2 exceptional gauge group [25–27,31,47–50].

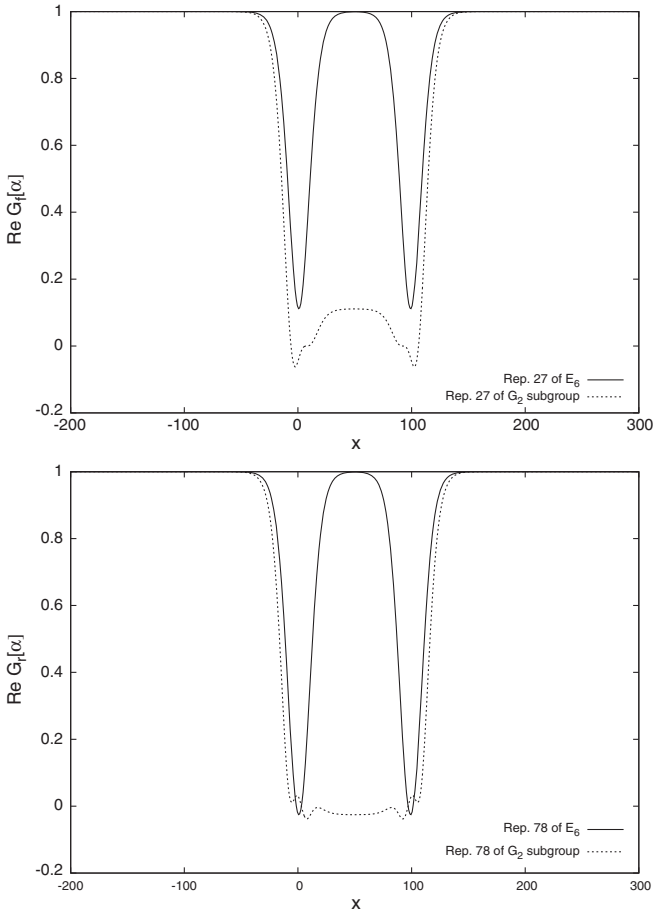

FIG. 17. The same as Fig. 15 but the dashed lines represent the group factor of the G_2 subgroup.

In Refs. [28–30], the static potentials of the G_2 exceptional gauge group have been investigated, and the dominant role of nontrivial center elements of its $SU(2)$ and $SU(3)$ subgroups on the intermediate confinement has been studied. In this research, we are going to insert our generalized method to calculate the potentials of higher representations of G_2 as well.

To begin, one needs the original Cartan generators of the G_2 exceptional group to simulate the static potential using the vacuum domain structure model. The Cartan generators of G_2 in the fundamental seven-dimensional representation are as follows [28,46]:

$$
\begin{aligned}
h_1^7 &= \frac{1}{2\sqrt{2}}\mathrm{diag}[+1, -1, 0, 0, -1, +1, 0],\\
h_2^7 &= \frac{1}{2\sqrt{6}}\mathrm{diag}[+1, +1, -2, 0, -1, -1, +2].
\end{aligned} \tag{93}
$$

These matrices are normalized with the Eq. (17) condition. Plotting the potential of Eq. (10) requires the group factor

in Eq. (3) and the flux profile in Eq. (7). In order to compute the maximum value of the flux profile, one has to apply the trivial flux condition in Eq. (19) and solve three independent equations:

$$\begin{aligned}\exp\left[\frac{\alpha^7_{\max_1}}{2\sqrt{2}}+\frac{\alpha^7_{\max_2}}{2\sqrt{6}}\right]&=\mathbb{I},\\ \exp\left[\frac{-\alpha^7_{\max_1}}{2\sqrt{2}}+\frac{\alpha^7_{\max_2}}{2\sqrt{6}}\right]&=\mathbb{I},\\ \exp\left[\frac{-\alpha^7_{\max_2}}{\sqrt{6}}\right]&=\mathbb{I},\end{aligned}\tag{94}$$

to find

$$\begin{aligned}\alpha^7_{\max_1}&=2\pi\sqrt{2},\\ \alpha^7_{\max_2}&=2\pi\sqrt{6}.\end{aligned}\tag{95}$$

It can be easily shown that the first Cartan generator h^7_1 in Eq. (93), with the maximum flux value of $\alpha^{\max}_1=4\pi\sqrt{2}$, is capable of producing the whole G_2 potential individually, without using h^7_2. In the next stage, we are going to calculate reconstructed Cartan generators in 7-, 14-, 27-, 64-, 77-, and 77′-dimensional representations from the decomposition of G_2 into its $SU(3)$ subgroup.

1. $SU(3)$ subgroup

The decomposition of the fundamental representation into the $SU(3)$ subgroup is as follows [36,37]:

$$\begin{aligned}&G_2\supset SU(3)\quad(R)\\ &7=3\oplus\bar{3}\oplus 1.\end{aligned}\tag{96}$$

The reconstructed Cartan generator with respect to this decomposition is

$$H^7_a=\frac{1}{\sqrt{2}}\mathrm{diag}[\lambda^3_a,-(\lambda^3_a)^*,0],\tag{97}$$

with $a=3,\ 8$. It is clear that the decomposition of this representation into the $SU(3)$ subgroup results in the same matrices as Eq. (93). Similar to the F_4 and E_6 exceptional groups, one is able to use $SU(3)$ subgroups to reproduce the group potentials. This matter enables us to calculate the potentials of higher representations by taking the same procedure. The decomposition of the higher representations of G_2 into the $SU(3)$ subgroup is [37]

$$\begin{aligned}14&=3\oplus\bar{3}\oplus 8,\\ 27&=8\oplus 6\oplus\bar{6}\oplus 3\oplus\bar{3}\oplus 1,\\ 64&=15\oplus\bar{15}\oplus 8\oplus 8\oplus 6\oplus\bar{6}\oplus 3\oplus\bar{3},\\ 77&=27\oplus 15\oplus\bar{15}\oplus 8\oplus 6\oplus\bar{6},\\ 77'&=15\oplus\bar{15}\oplus 10\oplus\bar{10}\oplus 8\oplus 6\oplus\bar{6}\oplus 3\oplus\bar{3}\oplus 1.\end{aligned}\tag{98}$$

So, the corresponding Cartan generators are decomposed as follows:

$$\begin{aligned}H^{14}_a&=\frac{1}{\sqrt{8}}\mathrm{diag}[\lambda^3_a,-(\lambda^3_a)^*,\lambda^8_a],\\ H^{27}_a&=\frac{1}{\sqrt{18}}\mathrm{diag}[\lambda^8_a,\lambda^6_6,-(\lambda^6_a)^*,\lambda^3_a,-(\lambda^3_a)^*,0],\\ H^{64}_a&=\frac{1}{8}\mathrm{diag}[\lambda^{15}_a,-(\lambda^{15}_a)^*,\lambda^8_a,\lambda^8_a,\lambda^6_a,-(\lambda^6_a)^*,\lambda^3_a,\\ &\quad-(\lambda^3_a)^*],\\ H^{77}_a&=\frac{1}{\sqrt{110}}\mathrm{diag}[\lambda^{27}_a,\lambda^{15}_a,-(\lambda^{15}_a)^*,\lambda^8_a,\lambda^6_a,-(\lambda^6_a)^*],\\ H^{77'}_a&=\frac{1}{2\sqrt{22}}\mathrm{diag}[\lambda^{15}_a,-(\lambda^{15}_a)^*,\lambda^{10}_a,-(\lambda^{10}_a)^*,\lambda^8_a,\\ &\quad\lambda^6_a,-(\lambda^6_a)^*,\lambda^3_a,-(\lambda^3_a)^*,0],\end{aligned}\tag{99}$$

where the upper indices of the λ_a's indicate the dimensions of the $SU(3)$ representations. The maximum flux values extracted from Eq. (19) are

$$\begin{aligned}\alpha^{14}_{\max_1}&=2\pi\sqrt{8}, &\alpha^{14}_{\max_2}&=2\pi\sqrt{24},\\ \alpha^{27}_{\max_1}&=6\pi\sqrt{2}, &\alpha^{27}_{\max_2}&=6\pi\sqrt{6},\\ \alpha^{64}_{\max_1}&=16\pi, &\alpha^{64}_{\max_2}&=16\pi\sqrt{3},\\ \alpha^{77}_{\max_1}&=2\pi\sqrt{110}, &\alpha^{77}_{\max_2}&=2\pi\sqrt{330},\\ \alpha^{77'}_{\max_1}&=4\pi\sqrt{22}, &\alpha^{77'}_{\max_2}&=4\pi\sqrt{66}.\end{aligned}\tag{100}$$

The trivial static potentials of Eq. (10) for the fundamental, adjoint, 27-, 64-, 77-, and 77′-dimensional representations have been plotted in Fig. 18. Screening is observed for all representations, which is a consequence of the adjoint "gluons" that pop out of the vacuum due to high energies and screen the initial color sources. The tensor products of all representations, when they create a singlet, are an implication of this phenomenon:

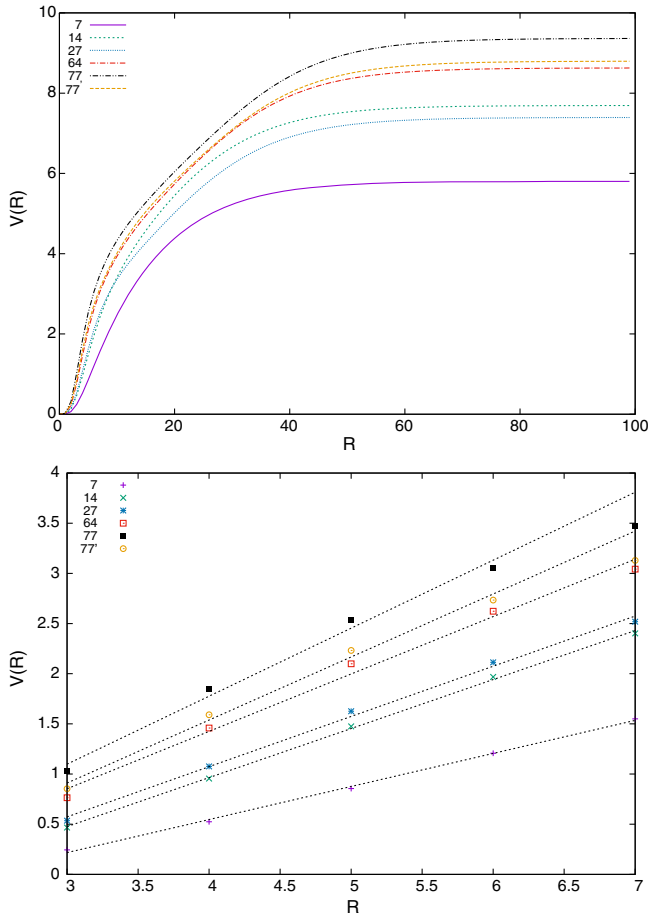

FIG. 18. Upper diagram: Static potentials of the G_2 exceptional group for the fundamental, adjoint, 27, 64, 77, and 77′ representations in the range $R \in [1, 100]$. All potentials are screened at far distances and are linear at intermediate distance scales. Lower diagram: Linear parts of the potentials in the range [3,7]. The slopes of the potentials are given in the fourth column of Table III.

$$
\begin{aligned}
7 \times 14 \times 14 \times 14 &= \mathbf{1} \oplus 10(7) \oplus 6(14) \oplus \cdots, \\
14 \times 14 &= \mathbf{1} \oplus 14 \oplus 27 \oplus \cdots, \\
27 \times 14 \times 14 &= \mathbf{1} \oplus 3(7) \oplus 3(14) \oplus \cdots, \\
64 \times 14 \times 14 \times 14 &= 2(\mathbf{1}) \oplus 20(7) \oplus \cdots, \\
77 \times 14 \times 14 &= \mathbf{1} \oplus 2(7) \oplus 4(14) \oplus \cdots, \\
77' \times 14 \times 14 &= \mathbf{1} \oplus 3(14) \oplus 3(27) \oplus \cdots. \qquad (101)
\end{aligned}
$$

The lower diagram of Fig. 18 shows the linear parts of the potentials in the range $R \in [3, 7]$. The slopes of the linear potentials and the potential ratios ($\frac{k_r}{k_F}$) are listed in the fourth and fifth columns of Table III, respectively. Comparing $\frac{k_r}{k_F}$ values with the values of $\frac{C_r}{C_F}$ shows that potentials are in qualitative agreement with Casimir scaling. The point-by-point ratios of the potentials have been plotted in Fig. 19 in the range $R \in [1, 20]$. The potential ratios start at accurate Casimir ratios. However, they plummet considerably at larger distances of R. In fact, the potential ratios almost

TABLE III. The second column lists the Casimir numbers of several representations of the G_2 exceptional group [25–27,42]. The Casimir ratios, slopes of the potentials obtained from the lower diagram of Fig. 18, and the potential ratios are given in the third, fourth, and fifth columns, respectively. The numbers in the parentheses indicate the fit error.

Rep.	Casimir numbers	$\frac{C_r}{C_F}$	Potential slope	$\frac{k_r}{k_F}$
7	$\frac{1}{2}$	1	0.329(8)	1
14	1	2	0.488(8)	1.48(1)
27	$\frac{7}{6}$	2.33	0.50(2)	1.52(1)
64	$\frac{7}{4}$	3.5	0.57(3)	1.74(3)
77′	2	4	0.63(4)	1.91(4)
77	$\frac{5}{2}$	5	0.68(5)	2.06(5)

reach a plateau at $R \to \infty$. To investigate the reason why the potentials are linear at intermediate distances, we study the effects of the subgroups of G_2.

The G_2 exceptional group owns three direct maximal subgroups, which are presented in Table I. Like those of the F_4 and E_6 exceptional groups, the center elements of the $SU(3)$ subgroup are not a direct cause of intermediate confining potentials of G_2 in several representations. Hence, we do not give a detailed calculation for this subgroup, because the results are the same as those of F_4 and E_6. So, we study the other subgroup of G_2. It should be mentioned that $SU(2) \times SU(2)$ is a regular subgroup. Hence, it proves that these features do not appear exclusively for singular maximal subgroups.

2. $SU(2) \times SU(2)$ subgroup

Using this subgroup, the fundamental and adjoint representations can be decomposed as follows [36,37]:

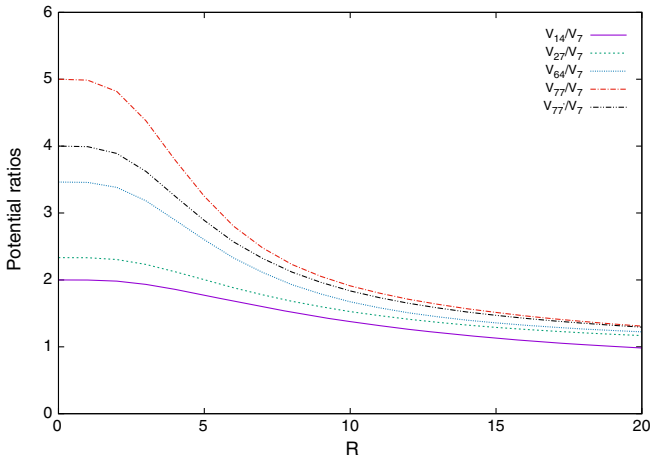

FIG. 19. Potential ratios in the different representations of the G_2 exceptional group that launch at exact Casimir ratios but deviate abruptly at farther distance ranges.

$$G_2 \supset SU(2) \times SU(2) \quad (R)$$
$$7 = (2,2) \oplus (1,3),$$
$$14 = (1,3) \oplus (3,1) \oplus (2,4). \tag{102}$$

Therefore, the reconstructed diagonal matrices for the fundamental and adjoint representations of G_2 with respect to the $SU(2) \times SU(2)$ subgroup are

$$H^7_{SU(2)} = \frac{1}{\sqrt{6}}\mathrm{diag}[\sigma_3^2, \sigma_3^2, \sigma_3^3],$$
$$H^{14}_{SU(2)} = \frac{1}{2\sqrt{6}}\mathrm{diag}[\sigma_3^3, 0, 0, 0, \sigma_3^4, \sigma_3^4]. \tag{103}$$

It is seen that the elements of these matrices are not identical to H_3^7 and H_3^{14} in Eqs. (96) and (98), respectively. Therefore, the trivial potentials obtained from this decomposition are not the same as the original ones for G_2. Nevertheless, the center element matrix of the $SU(2)$ subgroup is

$$\mathbb{Z}^7_{SU(2)} = [z_1 \mathbb{I}_{2\times2}, z_1 \mathbb{I}_{2\times2}, \mathbb{I}_{3\times3}],$$
$$\mathbb{Z}^{14}_{SU(2)} = [\mathbb{I}_{3\times3}, 1, 1, 1, z_1 \mathbb{I}_{4\times4}, z_1 \mathbb{I}_{4\times4}]. \tag{104}$$

So, if one uses the nontrivial maximum flux condition in Eq. (6), the nontrivial maximum flux values are

$$\alpha^{7\text{-non}}_{\text{max-SU(2)}} = 2\pi\sqrt{6},$$
$$\alpha^{14\text{-non}}_{\text{max-SU(2)}} = 2\pi\sqrt{24}. \tag{105}$$

The group factor function of the fundamental and adjoint representations obtained from this decomposition have been illustrated in Fig. 20, as well as the corresponding ones for G_2. The detailed calculation for the higher representations has been given in Appendix C. In this figure, the minimum points of the G_2 group factor, which occur at $x = 0$ and $x = 100$, reach the values -0.142 and -0.143 for the fundamental and adjoint representations, respectively. The corresponding group factors of the $SU(2) \times SU(2)$ subgroup reach the same amounts at $x = 50$. Therefore, similar to the F_4 and E_6 cases, the nontrivial center of the $SU(2)$ subgroup induces temporary confinement in the G_2 exceptional group.

Now, we go one step further and decompose the $SU(3)$ subgroup into its $SU(2)$ subgroup. This decomposition enables us to give a comprehensive conclusion from this work.

3. $SU(3) \supset SU(2) \times U(1)$ subgroup

The decomposition of the fundamental and adjoint representations of G_2 into the $SU(3)$ subgroup are

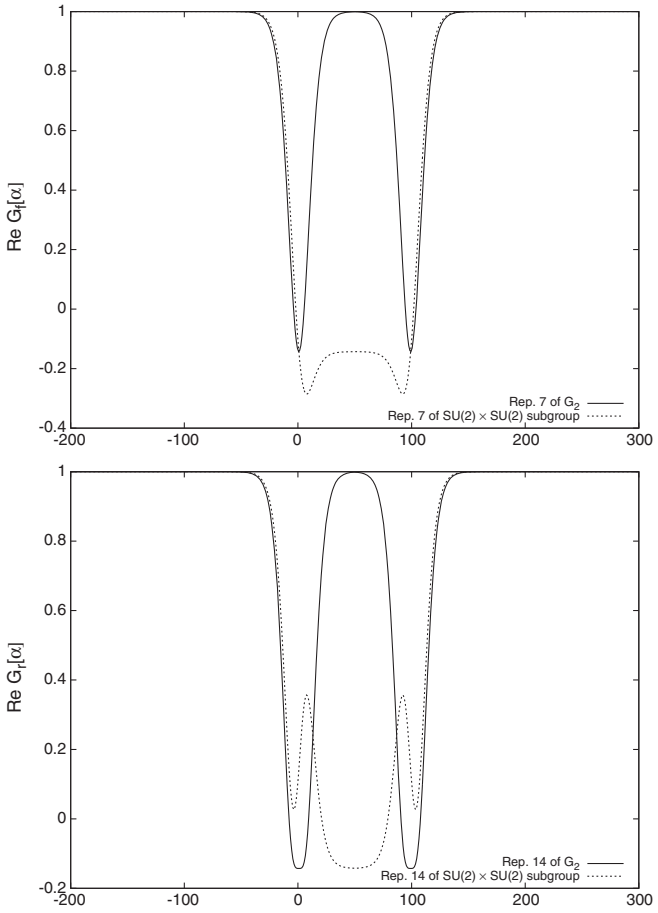

FIG. 20. The real part of the group factor function versus the location x of the vacuum domain midpoint, for $R = 100$ and in the range $x \in [-200, 300]$, for the fundamental and adjoint representation of G_2 (solid lines) in comparison with the same function versus the location x of the vortex midpoint obtained from the $SU(2) \times SU(2)$ decomposition (dashed lines). The minimum points of the G_2 group factor, which occur at $x = 0$ and $x = 100$, reach the amounts -0.142 and -0.143 for the fundamental and adjoint representations, respectively.

$$G_2 \supset SU(3)$$
$$7 = 3 \oplus \bar{3} \oplus 1,$$
$$14 = 3 \oplus \bar{3} \oplus 8. \tag{106}$$

In the next step,

$$SU(3) \supset SU(2) \times U(1) \quad (\mathrm{R})$$
$$3 = 2 \oplus 1,$$
$$8 = 3 \oplus 2 \oplus 2 \oplus 1. \tag{107}$$

It should be recalled that the $U(1)$ factor has been ignored in these decompositions. Ultimately, one could have

$$7 = 2 \oplus 1 \oplus 2 \oplus 1 \oplus 1,$$
$$14 = 2 \oplus 1 \oplus 2 \oplus 1 \oplus 3 \oplus 2 \oplus 2 \oplus 1. \quad (108)$$

Using the above decompositions, one is able to reconstruct the Cartan matrices for the fundamental and adjoint representations as follows:

$$H^{7}_{SU(3)\supset SU(2)} = \frac{1}{\sqrt{2}}\mathrm{diag}[\sigma_3^2, 0, \sigma_3^2, 0, 0],$$
$$H^{14}_{SU(3)\supset SU(2)} = \frac{1}{2\sqrt{2}}\mathrm{diag}[\sigma_3^2, 0, \sigma_3^2, 0, \sigma_3^3, \sigma_3^2, \sigma_3^2, 0]. \quad (109)$$

We are going to investigate the role of this decomposition in the intermediate linear potentials of G_2. So, the matrices of the center elements are calculated as

$$\mathbb{Z}^{7}_{SU(3)\supset SU(2)} = \mathrm{diag}[z_1\mathbb{I}_{2\times2}, 1, z_1\mathbb{I}_{2\times2}, 1, 1],$$
$$\mathbb{Z}^{14}_{SU(3)\supset SU(2)} = \mathrm{diag}[z_1\mathbb{I}_{2\times2}, 1, z_1\mathbb{I}_{2\times2}, 1, \mathbb{I}_{3\times3}, z_1\mathbb{I}_{2\times2}, z_1\mathbb{I}_{2\times2}, 1]. \quad (110)$$

Using the maximum flux condition in Eq. (6), we find

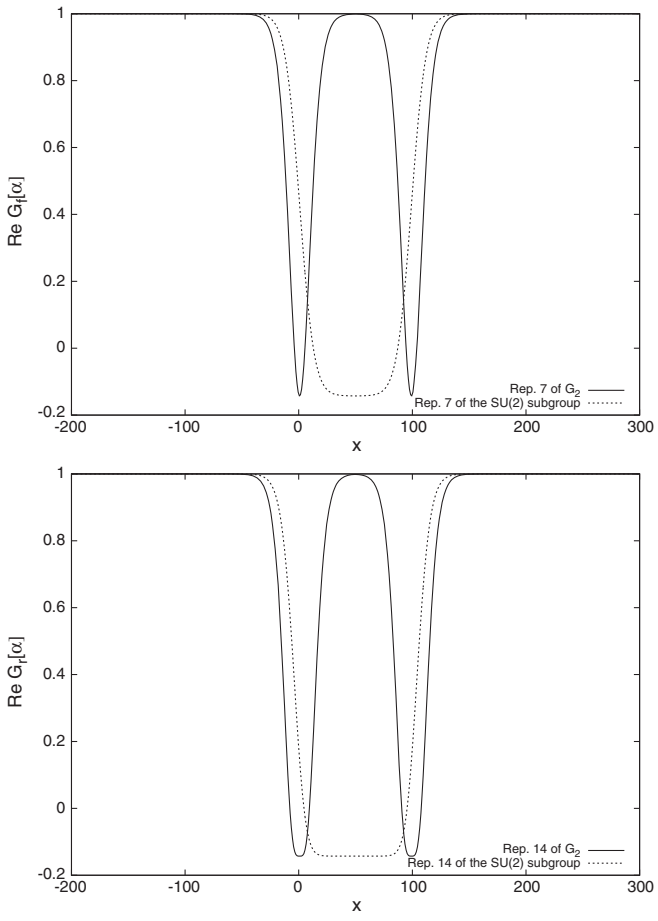

FIG. 21. The same as Fig. 20 but the dashed lines represent the group factor for the $SU(3) \supset SU(2) \times U(1)$ decomposition.

$$\alpha_{\max}^{7\text{-non}} = 2\pi\sqrt{2},$$
$$\alpha_{\max}^{14\text{-non}} = 4\pi\sqrt{2}. \quad (111)$$

The group factor function of the fundamental and adjoint representations obtained from this decomposition have been illustrated in Fig. 21, as well as the corresponding ones for G_2. It is observed that in each diagram the minimum values of the two graphs are identical. Hence, the $SU(2)$ gauge group has a dominant role in the linear part of the trivial potentials of the exceptional gauge groups.

V. CONCLUSION

In this article, we have presented a generalized scenario whereby the static potentials in different representations of exceptional gauge groups could be calculated by means of their unit center elements in the framework of the vacuum domain structure model. Although G_2 and F_4 exceptional groups do not possess any nontrivial center elements and confinement is not expected, linear potential is observed for all representations at intermediate distances. This fact is also correct for the E_6 exceptional gauge group, when one uses only the trivial center element in the calculation. In addition, to calculate these types of trivial potentials, there is no need to use all the Cartan generators of the gauge group. For example, concerning the G_2, F_4, and E_6 exceptional groups, it seems adequate to consider only their first Cartan generators, which are h_1^7, h_1^{26}, and h_1^{27} in their fundamental representations, respectively. On the other hand, if the Cartan generators reconstructed by the group decomposition into the maximal subgroups have the same elements as h_1, they are able to simulate the exact static potentials as the exceptional supergroups, themselves. Thus, one is able to apply these subgroup decompositions to gain the static potential of the higher representations of the exceptional groups. Hence, Casimir scaling of different representations of these groups is observed. This method is not applicable for the potentials obtained by the nontrivial center elements of E_6; i.e., the potentials calculated by the nontrivial center elements in the thick center vortex model are not identical to the potentials of their subgroups. Hence, it seems that this method is just valid when we use only the unit center element of the gauge groups to calculate the static potentials.

To find the reason for the temporary confinement at intermediate distances, we have turned to the center elements of the $SU(N)$ subgroups by which their center vortices indirectly produce the intermediate linear part in the supergroups. So, the group factor function $\mathrm{Re}\mathcal{G}_r[\vec{\alpha}(x)]$ has been investigated in different representations of the G_2, F_4, and E_6 exceptional gauge groups using the unit center element only. Comparison of this function with the corresponding one obtained from the nontrivial center elements of the $SU(N)$ subgroups shows that the center vortices of

the $SU(3)$ subgroups in none of these exceptional groups could be responsible for the intermediate linear potential, since the group factor functions reach different minimum amounts. However, by means of the trivial center element of this subgroup, the same potential as the exceptional group itself is produced.

Any regular or singular decomposition into the $SU(2)$ subgroup that produces a Cartan generator with the same elements as h_1 gives rise to the linear intermediate parts in the potentials of the supergroups. In fact, the extremums of $\mathrm{Re}\mathcal{G}_r[\vec{\alpha}(x)]$, which occur at the points where 50% of the vacuum domain flux enters the Wilson loop, are responsible for the intermediate linear potential. When the center element obtained from these $SU(2)$ decompositions lies entirely inside the Wilson loop, the corresponding group factor reaches a value that is equal to the extremum values of $\mathrm{Re}\mathcal{G}_r[\vec{\alpha}(x)]$ for the given exceptional group.

Furthermore, there are some subgroups such as $SU(2)\times SU(2)$ for G_2 and $SU(2)\times G_2$ for the F_4 and G_2 singular subgroup of E_6 that produce different potentials from their supergroup. Yet, they are responsible for the temporary confinement in different representations. In fact, if the number of center elements or center vortices in the matrix of center elements obtained from two different decompositions is the same, the corresponding group factors reach the same value when the vortex is located completely inside the Wilson loop. The dominant role of the $SU(2)$ subgroup in observing the temporary confinement obtained by the unit center element is not exclusive to the exceptional gauge groups. In the next work, we argue that this dominant role of the $SU(2)$ subgroup is seen for the trivial potentials of the $SU(N)$ gauge groups as well. We should mention that, due to the oversimplification of the model, the results that have been presented in this paper seem to be restricted in the framework of the vacuum domain structure and thick center vortex models.

APPENDIX A: $F_4 \supset SU(3)\times SU(3)$

The decompositions of 273- and 324-dimensional irreps of F_4 to the irreps of the $SU(3)\times SU(3)$ subgroup are as follows [36,37]:

$$\begin{aligned}273 = {} & (1,1)\oplus(8,1)\oplus(3,3)\oplus(\bar{3},\bar{3})\oplus(10,1)\oplus(\bar{10},1)\oplus(6,\bar{3})\oplus(\bar{6},3)\oplus(3,\bar{6})\oplus(\bar{3},6)\\ & \oplus(15,3)\oplus(\bar{15},\bar{3})\oplus(8,8),\end{aligned} \tag{A1}$$

$$\begin{aligned}324 = {} & (1,1)\oplus(8,1)\oplus(1,8)\oplus(\bar{3},\bar{3})\oplus(3,3)\oplus(6,\bar{3})\oplus(\bar{6},3)\oplus(27,1)\oplus(\bar{6},\bar{6})\oplus(6,6)\oplus(15,3)\\ & \oplus(\bar{15},\bar{3})\oplus(8,8).\end{aligned} \tag{A2}$$

Thus, the Cartan diagonal generators reconstructed by taking advantage of Eqs. (A1) and (A2) are

$$\begin{aligned}H_a^{273} = {} & \frac{1}{3\sqrt{14}}\mathrm{diag}[0,\overbrace{0,\ldots,0}^{8\,\text{times}},\lambda_a^3,\lambda_a^3,\lambda_a^3,-(\lambda_a^3)^*,-(\lambda_a^3)^*,-(\lambda_a^3)^*,\overbrace{0,\ldots,0}^{10\,\text{times}},\overbrace{0,\ldots,0}^{10\,\text{times}},\\ & \overbrace{-(\lambda_a^3)^*,\ldots,-(\lambda_a^3)^*}^{6\,\text{times}},,\overbrace{\lambda_a^3,\ldots,\lambda_a^3}^{6\,\text{times}},-(\lambda_a^6)^*,-(\lambda_a^6)^*,-(\lambda_a^6)^*,\lambda_a^6,\lambda_a^6,\lambda_a^6,\overbrace{\lambda_a^3,\ldots,\lambda_a^3}^{15\,\text{times}},,\overbrace{-(\lambda_a^3)^*,\ldots,-(\lambda_a^3)^*}^{15\,\text{times}},\overbrace{\lambda_a^8,\ldots,\lambda_a^8}^{8\,\text{times}}],\end{aligned} \tag{A3}$$

$$\begin{aligned}H_a^{324} = {} & \frac{1}{9\sqrt{2}}\mathrm{diag}[0,\overbrace{0,\ldots,0}^{8\,\text{times}},\lambda_a^8,\overbrace{\lambda_a^3,\ldots,\lambda_a^3}^{3\,\text{times}},\overbrace{-(\lambda_a^3)^*,\ldots,-(\lambda_a^3)^*}^{3\,\text{times}},\overbrace{(\lambda_a^3)^*,\ldots,-(\lambda_a^3)^*}^{6\,\text{times}},\overbrace{\lambda_a^3,\ldots,\lambda_a^3}^{6\,\text{times}},\\ & \overbrace{0,\ldots,0}^{27\,\text{times}},\overbrace{-(\lambda_a^6)^*,\ldots,-(\lambda_a^6)^*}^{6\,\text{times}},\overbrace{\lambda_a^6,\ldots,\lambda_a^6}^{6\,\text{times}},\overbrace{\lambda_a^3,\ldots,\lambda_a^3}^{15\,\text{times}},\overbrace{-(\lambda_a^3)^*,\ldots,-(\lambda_a^3)^*}^{15\,\text{times}},\overbrace{\lambda_a^8,\ldots,\lambda_a^8}^{8\,\text{times}}].\end{aligned} \tag{A4}$$

Using the trivial flux condition in Eq. (19), the maximum flux values are calculated as follows:

$$\alpha_{max_1}^{273} = 6\pi\sqrt{14}, \qquad \alpha_{max_2}^{273} = 6\pi\sqrt{42}, \qquad \alpha_{max_1}^{324} = 18\pi\sqrt{2}, \qquad \alpha_{max_2}^{324} = 18\pi\sqrt{6}. \tag{A5}$$

The static potential calculated by means of the above equations has been given in Fig. 6. We can build up the center element matrices:

$$\mathbb{Z}^{273}_{SU(3)} = \mathrm{diag}[1, \overbrace{1,\ldots,1}^{8\text{ times}}, \overbrace{z_n\mathbb{I}_{3\times3},\ldots,z_n\mathbb{I}_{3\times3}}^{3\text{ times}}, \overbrace{z_n^*\mathbb{I}_{3\times3},\ldots,z_n^*\mathbb{I}_{3\times3}}^{3\text{ times}}, \overbrace{1,\ldots,1}^{10\text{ times}}, \overbrace{1,\ldots,1}^{10\text{ times}}, \overbrace{z_n\mathbb{I}_{3\times3},\ldots,z_n\mathbb{I}_{3\times3}}^{6\text{ times}}, \overbrace{z_n^*\mathbb{I}_{3\times3},\ldots,z_n^*\mathbb{I}_{3\times3}}^{6\text{ times}},$$
$$\overbrace{z_n^*\mathbb{I}_{6\times6},\ldots,z_n^*\mathbb{I}_{6\times6}}^{3\text{ times}}, \overbrace{z_n\mathbb{I}_{6\times6},\ldots,z_n\mathbb{I}_{6\times6}}^{3\text{ times}}, \overbrace{z_n\mathbb{I}_{3\times3},\ldots,z_n\mathbb{I}_{3\times3}}^{15\text{ times}}, \overbrace{z_n^*\mathbb{I}_{3\times3},\ldots,z_n^*\mathbb{I}_{3\times3}}^{15\text{ times}}, \overbrace{\mathbb{I}_{8\times8},\ldots,\mathbb{I}_{8\times8}}^{8\text{ times}}], \tag{A6}$$

$$\mathbb{Z}^{324}_{SU(3)} = \mathrm{diag}[1, \overbrace{1,\ldots,1}^{8\text{ times}}, \mathbb{I}_{8\times8}\overbrace{z_n^*\mathbb{I}_{3\times3},\ldots,z_n^*\mathbb{I}_{3\times3}}^{3\text{ times}}, \overbrace{z_n\mathbb{I}_{3\times3},\ldots,z_n\mathbb{I}_{3\times3}}^{3\text{ times}}, \overbrace{z_n^*\mathbb{I}_{3\times3},\ldots,z_n^*\mathbb{I}_{3\times3}}^{6\text{ times}}, \overbrace{z_n\mathbb{I}_{3\times3},\ldots,z_n\mathbb{I}_{3\times3}}^{6\text{ times}},$$
$$\overbrace{1,\ldots,1}^{27\text{ times}}, \overbrace{z_n^*\mathbb{I}_{6\times6},\ldots,z_n^*\mathbb{I}_{6\times6}}^{6\text{ times}}, \overbrace{z_n\mathbb{I}_{6\times6},\ldots,z_n\mathbb{I}_{6\times6}}^{6\text{ times}}, \overbrace{z_n\mathbb{I}_{3\times3},\ldots,z_n\mathbb{I}_{3\times3}}^{15\text{ times}}, \overbrace{z_n^*\mathbb{I}_{3\times3},\ldots,z_n^*\mathbb{I}_{3\times3}}^{15\text{ times}}, \overbrace{\mathbb{I}_{8\times8},\ldots,\mathbb{I}_{8\times8}}^{8\text{ times}}]. \tag{A7}$$

Then, we use the nontrivial flux profile condition of Eq. (6) to estimate the maximum flux values for these representations:

$$\alpha^{273-\mathrm{non}}_{\mathrm{max}_1} = 6\pi\sqrt{14} \qquad \alpha^{273-\mathrm{non}}_{\mathrm{max}_2} = 2\pi\sqrt{42} \qquad \alpha^{324-\mathrm{non}}_{\mathrm{max}_1} = 18\pi\sqrt{2} \qquad \alpha^{324-\mathrm{non}}_{\mathrm{max}_2} = 6\pi\sqrt{6}. \tag{A8}$$

Accordingly, using Eqs. (A2)–(A4) and (A8), the group factor functions could be plotted in Fig. 22.

APPENDIX B: $F_4 \supset SO(9) \supset SU(2) \times SU(4)$

Representations 273 and 324 of the F_4 exceptional group can be decomposed to the representations of the $SO(9)$ subgroup as follows:

$$F_4 \supset SO(9) \qquad 273 = 9 \oplus 16 \oplus 36 \oplus 84 \oplus 128,$$
$$324 = 1 \oplus 9 \oplus 16 \oplus 44 \oplus 126 \oplus 128. \tag{B1}$$

In the next step,

$$\begin{aligned} SO(9) &\supset SU(2) \times SU(4) \\ 9 &= (3,1) \oplus (1,6), \\ 16 &= (2,4) \oplus (2,\bar{4}), \\ 36 &= (3,1) \oplus (1,15) \oplus (3,6), \\ 44 &= (1,1) \oplus (5,1) \oplus (3,6) \oplus (1,20'), \\ 84 &= (1,1) \oplus (1,10) \oplus (1,\bar{10}) \oplus (3,6) \oplus (3,15), \\ 126 &= (1,6) \oplus (3,10) \oplus (3,\bar{10}) \oplus (1,15) \oplus (3,15), \\ 128 &= (2,4) \oplus (2,\bar{4}) \oplus (4,4) \oplus (4,\bar{4}) \oplus (2,20) \\ &\quad \oplus (2,\bar{20}). \end{aligned} \tag{B2}$$

Now, we decompose $SU(4)$ into its $SU(2)$ subgroup:

$$\begin{aligned} SU(4) &\supset SU(2) \times SU(2) \times U(1), \qquad 4 = (2,1) \oplus (1,2), \\ 6 &= (1,1) \oplus (1,1) \oplus (2,2), \\ 10 &= (2,2) \oplus (3,1) \oplus (1,3), \\ 15 &= (1,1) \oplus (2,2) \oplus (2,2) \oplus (3,1) \oplus (1,3), \\ 20 &= (2,1) \oplus (2,1) \oplus (1,2) \oplus (1,2) \oplus (3,2) \oplus (2,3), \\ 20' &= (1,1) \oplus (1,1) \oplus (1,1) \oplus (2,2) \oplus (2,2) \oplus (3,3). \end{aligned} \tag{B3}$$

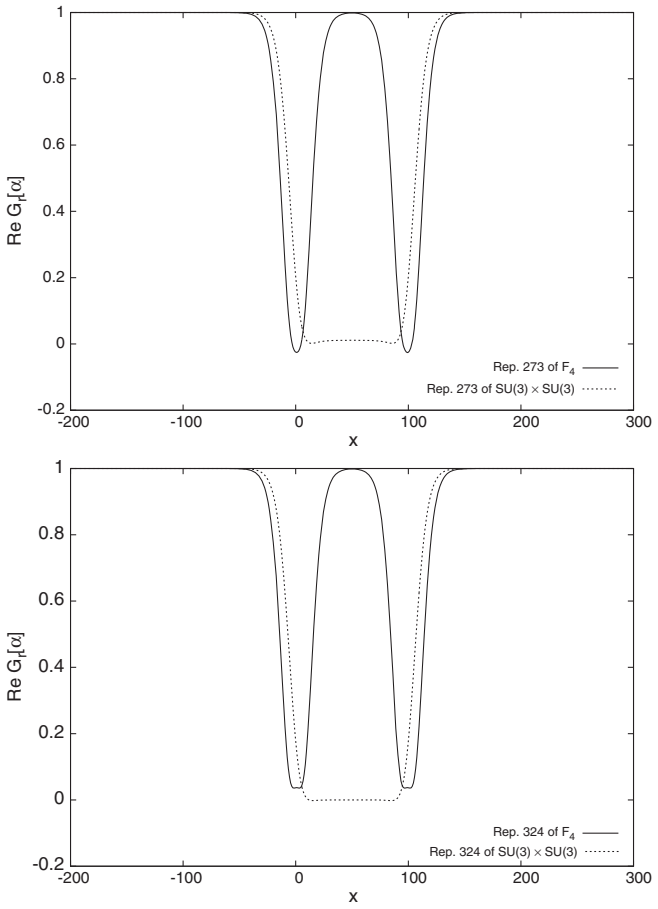

FIG. 22. The same as Fig. 8 but for representations 273 and 324. The minimum values of the F_4 group factor for representations 273 and 324 are -0.025 and 0.037, respectively. It is seen that the minimum values of the group factors for the $SU(3) \times SU(3)$ decomposition are not identical to the corresponding ones for F_4.

Ultimately we have

$$273 = \overbrace{(1,1)\oplus\cdots\oplus(1,1)}^{19\text{ times}} \oplus \overbrace{(3,1)\oplus\cdots\oplus(3,1)}^{8\text{ times}} \oplus \overbrace{(2,2)\oplus\cdots\oplus(2,2)}^{17\text{ times}} \oplus \overbrace{(2,1)\oplus\cdots\oplus(2,1)}^{24\text{ times}} \oplus \overbrace{(1,2)\oplus\cdots\oplus(1,2)}^{24\text{ times}} \oplus \overbrace{(1,3)\oplus\cdots\oplus(1,3)}^{6\text{ times}} \oplus \overbrace{(2,3)\oplus\cdots\oplus(2,3)}^{4\text{ times}} \oplus \overbrace{(3,2)\oplus\cdots\oplus(3,2)}^{4\text{ times}} \tag{B4}$$

$$324 = 1 \oplus \overbrace{(1,1)\oplus\cdots\oplus(1,1)}^{18\text{ times}} \oplus \overbrace{(3,1)\oplus\cdots\oplus(3,1)}^{11\text{ times}} \oplus \overbrace{(2,2)\oplus\cdots\oplus(2,2)}^{21\text{ times}} \oplus \overbrace{(2,1)\oplus\cdots\oplus(2,1)}^{24\text{ times}} \oplus \overbrace{(1,2)\oplus\cdots\oplus(1,2)}^{24\text{ times}} \oplus \overbrace{(1,3)\oplus\cdots\oplus(1,3)}^{10\text{ times}} \oplus \overbrace{(2,3)\oplus\cdots\oplus(2,3)}^{4\text{ times}} \oplus \overbrace{(3,2)\oplus\cdots\oplus(3,2)}^{4\text{ times}} \oplus (3,3) \oplus (5,1) \tag{B5}$$

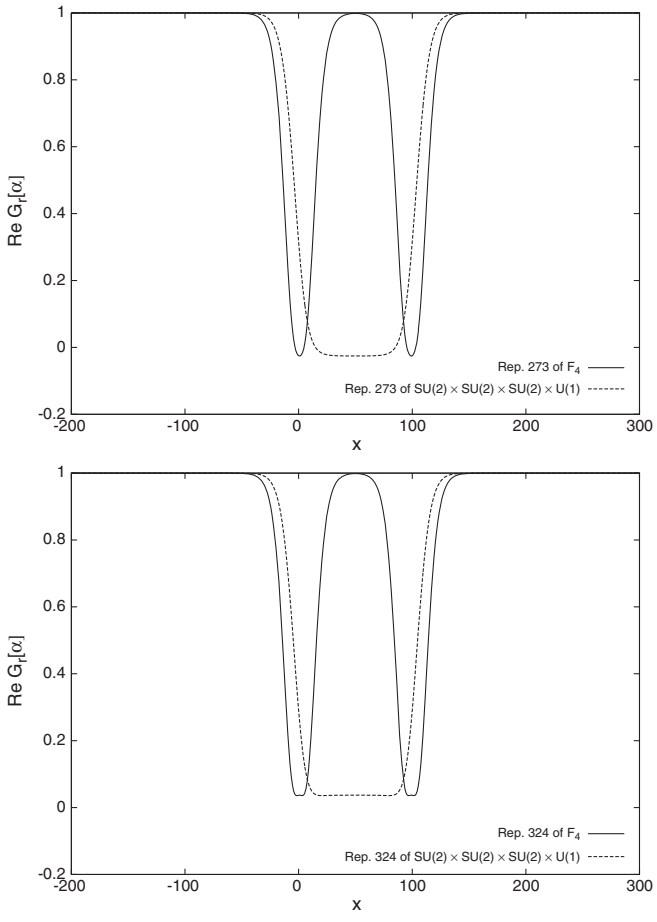

FIG. 23. The real part of the group factor versus the location x of the vacuum domain midpoint, for $R = 100$ and in the range $x \in [-200, 300]$, for representations 273 and 324 of F_4 (solid lines) in comparison with the one obtained from the $SO(9) \supset SU(2) \times SU(4)$ decomposition using its nontrivial center elements (dashed lines). In each diagram, the minimum values are identical.

and

$$H^{273}_{SU(2)} = \frac{1}{3\sqrt{14}}\,\mathrm{diag}[\overbrace{0,\ldots,0}^{91\text{ times}}, \overbrace{\sigma_3^2,\ldots,\sigma_3^2}^{70\text{ times}}, \overbrace{\sigma_3^3,\ldots,\sigma_3^3}^{14\text{ times}}],$$
$$H^{324}_{SU(2)} = \frac{1}{9\sqrt{2}}\,\mathrm{diag}[\overbrace{0,\ldots,0}^{105\text{ times}}, \overbrace{\sigma_3^2,\ldots,\sigma_3^2}^{78\text{ times}}, \overbrace{\sigma_3^3,\ldots,\sigma_3^3}^{21\text{ times}}]. \tag{B6}$$

The matrices made of the center elements of the $SU(2)$ gauge group corresponding to the duality of its representation with respect to Eqs. (B4) and (B5) are as follows:

$$\mathbb{Z}^{273}_{SU(2)} = \mathrm{diag}[\overbrace{1,\ldots,1}^{91\text{ times}}, \overbrace{z_1\mathbb{I}_{2\times2},\ldots,z_1\mathbb{I}_{2\times2}}^{70\text{ times}}, \overbrace{\mathbb{I}_{3\times3},\ldots,\mathbb{I}_{3\times3}}^{14\text{ times}}],$$
$$\mathbb{Z}^{324}_{SU(2)} = \mathrm{diag}[\overbrace{1,\ldots,1}^{105\text{ times}}, \overbrace{z_1\mathbb{I}_{2\times2},\ldots,z_1\mathbb{I}_{2\times2}}^{78\text{ times}}, \overbrace{\mathbb{I}_{3\times3},\ldots,\mathbb{I}_{3\times3}}^{21\text{ times}}]. \tag{B7}$$

The maximum flux values could be calculated from the nontrivial flux condition of Eq. (6):

$$\alpha^{273\text{-non}}_{SU(2)\text{-max}} = 6\pi\sqrt{14}, \alpha^{324\text{-non}}_{SU(2)\text{-max}} = 18\pi\sqrt{2}. \tag{B8}$$

The group factor functions of these representations have been given in Fig. 23.

APPENDIX C: $G_2 \supset SU(2) \times SU(2)$

Decompositions of the G_2 representations into the $SU(2) \times SU(2)$ regular subgroup representations are

$$
\begin{aligned}
27 &= (3,3) \oplus (2,4) \oplus (2,2) \oplus (1,5) \oplus (1,1),\\
64 &= (4,2) \oplus (3,5) \oplus (3,3) \oplus (2,6) \oplus (2,4) \oplus (2,2) \oplus (1,5) \oplus (1,3),\\
77 &= (5,1) \oplus (4,4) \oplus (3,7) \oplus (3,3) \oplus (2,6) \oplus (2,4) \oplus (1,5) \oplus (1,1),\\
77' &= (4,4) \oplus (3,5) \oplus (3,3) \oplus (3,1) \oplus (2,6) \oplus (2,4) \oplus (2,2) \oplus (1,7) \oplus (1,3).
\end{aligned} \tag{C1}
$$

The Cartan generators could be reconstructed as follows:

$$
\begin{aligned}
H^{27}_{SU(2)} &= \frac{1}{3\sqrt{6}}\mathrm{diag}[\sigma_3^3,\sigma_3^3,\sigma_3^3,\sigma_3^4,\sigma_3^4,\sigma_3^2,\sigma_3^2,\sigma_3^5,0],\\
H^{64}_{SU(2)} &= \frac{1}{8\sqrt{3}}\mathrm{diag}[\sigma_3^2,\sigma_3^2,\sigma_3^2,\sigma_3^2,\sigma_3^5,\sigma_3^5,\sigma_3^5,\sigma_3^3,\sigma_3^3,\sigma_3^3,\sigma_3^6,\sigma_3^6,\sigma_3^4,\sigma_3^4,\sigma_3^2,\sigma_3^2,\sigma_3^5,\sigma_3^3],\\
H^{77}_{SU(2)} &= \frac{1}{\sqrt{330}}\mathrm{diag}[0,0,0,0,0,\sigma_3^4,\sigma_3^4,\sigma_3^4,\sigma_3^4,\sigma_3^7,\sigma_3^7,\sigma_3^7,\sigma_3^3,\sigma_3^3,\sigma_3^3,\sigma_3^6,\sigma_3^6,\sigma_3^4,\sigma_3^4,\sigma_3^5,0],\\
H^{77'}_{SU(2)} &= \frac{1}{2\sqrt{66}}\mathrm{diag}[\sigma_3^4,\sigma_3^4,\sigma_3^4,\sigma_3^4,\sigma_3^5,\sigma_3^5,\sigma_3^5,\sigma_3^3,\sigma_3^3,\sigma_3^3,0,0,0,\sigma_3^6,\sigma_3^6,\sigma_3^4,\sigma_3^4,\sigma_3^2,\sigma_3^2,\sigma_3^7,\sigma_3^3].
\end{aligned} \tag{C2}
$$

The center element matrices of the $SU(2)\times SU(2)$ subgroup are

$$
\begin{aligned}
\mathbb{Z}^{27}_{SU(2)} &= \mathrm{diag}[\mathbb{I}_{3\times3},\mathbb{I}_{3\times3},\mathbb{I}_{3\times3},z_1\mathbb{I}_{4\times4},z_1\mathbb{I}_{4\times4},z_1\mathbb{I}_{2\times2},z_1\mathbb{I}_{2\times2},\mathbb{I}_{5\times5},1],\\
\mathbb{Z}^{64}_{SU(2)} &= \mathrm{diag}[z_1\mathbb{I}_{2\times2},z_1\mathbb{I}_{2\times2},z_1\mathbb{I}_{2\times2},z_1\mathbb{I}_{2\times2},\mathbb{I}_{5\times5},\mathbb{I}_{5\times5},\mathbb{I}_{5\times5},\mathbb{I}_{3\times3},\mathbb{I}_{3\times3},\mathbb{I}_{3\times3},z_1\mathbb{I}_{6\times6},z_1\mathbb{I}_{6\times6},z_1\mathbb{I}_{4\times4},z_1\mathbb{I}_{4\times4},z_1\mathbb{I}_{2\times2},z_1\mathbb{I}_{2\times2},\mathbb{I}_{5\times5},\mathbb{I}_{3\times3}],\\
\mathbb{Z}^{77}_{SU(2)} &= \mathrm{diag}[1,1,1,1,1,z_1\mathbb{I}_{4\times4},z_1\mathbb{I}_{4\times4},z_1\mathbb{I}_{4\times4},z_1\mathbb{I}_{4\times4},\mathbb{I}_{7\times7},\mathbb{I}_{7\times7},\mathbb{I}_{7\times7},\mathbb{I}_{3\times3},\mathbb{I}_{3\times3},\mathbb{I}_{3\times3},z_1\mathbb{I}_{6\times6},z_1\mathbb{I}_{6\times6},z_1\mathbb{I}_{4\times4},z_1\mathbb{I}_{4\times4},\mathbb{I}_{5\times5},1],\\
\mathbb{Z}^{77'}_{SU(2)} &= \mathrm{diag}[z_1\mathbb{I}_{4\times4},z_1\mathbb{I}_{4\times4},z_1\mathbb{I}_{4\times4},z_1\mathbb{I}_{4\times4},\mathbb{I}_{5\times5},\mathbb{I}_{5\times5},\mathbb{I}_{5\times5},\mathbb{I}_{3\times3},\mathbb{I}_{3\times3},\mathbb{I}_{3\times3},1,1,\\
&\quad 1,z_1\mathbb{I}_{6\times6},z_1\mathbb{I}_{6\times6},z_1\mathbb{I}_{4\times4},z_1\mathbb{I}_{4\times4},z_1\mathbb{I}_{2\times2},z_1\mathbb{I}_{2\times2},\mathbb{I}_{7\times7},\mathbb{I}_{3\times3}].
\end{aligned} \tag{C3}
$$

Using the nontrivial maximum flux condition of Eq. (6), we find

$$
\alpha^{27\text{-non}}_{SU(2)\text{-max}} = 6\pi\sqrt{6}, \qquad \alpha^{64\text{-non}}_{SU(2)\text{-max}} = 16\pi\sqrt{3}, \qquad \alpha^{77\text{-non}}_{SU(2)\text{-max}} = 2\pi\sqrt{330}, \qquad \alpha^{77'\text{-non}}_{SU(2)\text{-max}} = 4\pi\sqrt{66}. \tag{C4}
$$

The group factor of representations 27, 64, 77, and 77′ have been presented in Figs. 24–27.

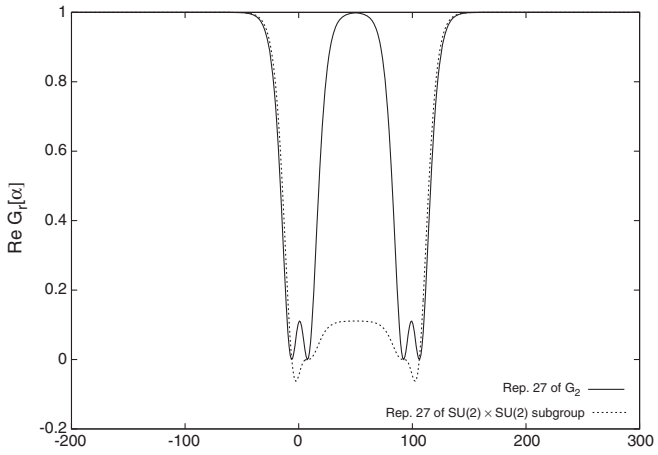

FIG. 24. The same as Fig. 20 but for representation 27. The extremum values of the F_4 group factor at $x = 0$ and $x = 100$ are approximately equal to 0.111.

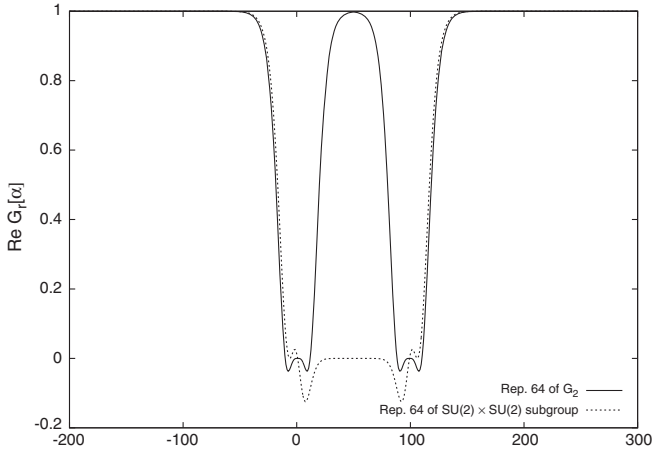

FIG. 25. The same as Fig. 20 but for representation 64. The extremum values of the F_4 group factor at $x = 0$ and $x = 100$ are approximately equal to 0.

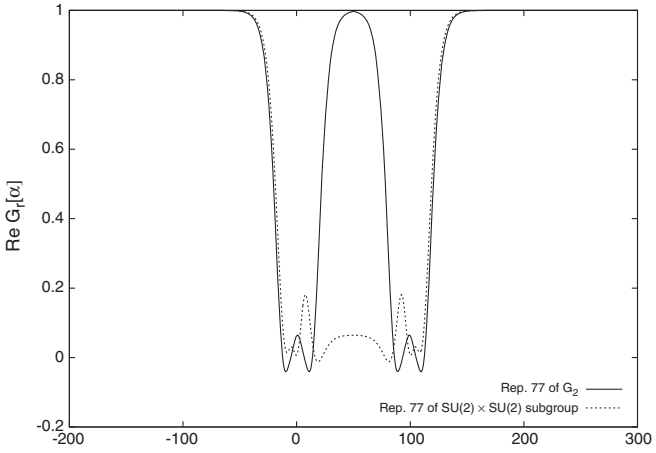

FIG. 26. The same as Fig. 20 but for representation 77. The extremum values of the F_4 group factor at $x = 0$ and $x = 100$ are approximately equal to 0.064.

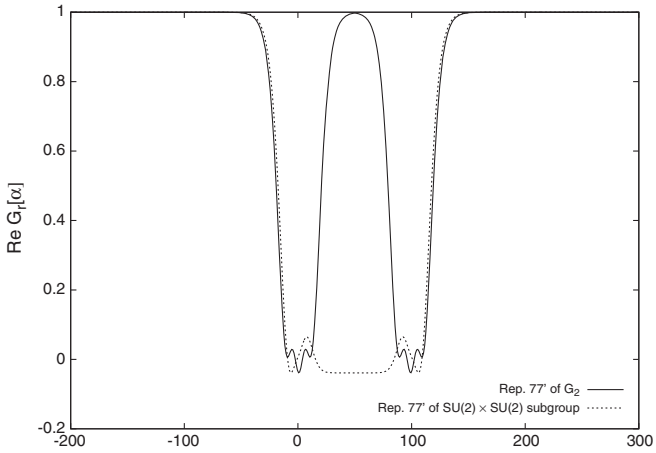

FIG. 27. The same as Fig. 20 but for representation 77′. The extremum values of the F_4 group factor at $x = 0$ and $x = 100$ are approximately equal to -0.038.

[1] G. 't Hooft, On the phase transition towards permanent quark confinement, Nucl. Phys. **B138**, 1 (1978).

[2] P. Vinciarelli, Fluxon solutions in non-Abelian gauge models, Phys. Lett. **78B**, 485 (1978).

[3] J. M. Cornwall, Quark confinement and vortices in massive gauge-invariant QCD, Nucl. Phys. **B157**, 392 (1979).

[4] R. P. Feynman, The qualitative behavior of Yang-Mills theory in 2+1 dimensions, Nucl. Phys. **B188**, 479 (1981).

[5] H. B. Nielsen and P. Olesen, A quantum liquid model for the QCD vacuum: Gauge and rotational invariance of domained and quantized homogeneous color fields, Nucl. Phys. **B160**, 380 (1979).

[6] J. Ambjørn and P. Olesen, On the formation of a random color magnetic quantum liquid in QCD, Nucl. Phys. **B170**, 60 (1980).

[7] J. Ambjørn and P. Olesen, A color magnetic vortex condensate in QCD, Nucl. Phys. **B170**, 265 (1980).

[8] J. Ambjørn, B. Felsager, and P. Olesen, Kinematics of periodic structures in SU(N) gauge theories, Nucl. Phys. **B175**, 349 (1980).

[9] P. Olesen, Confinement and random fluxes, Nucl. Phys. **B200**, 381 (1982).

[10] Y. Aharonov, A. Casher, and S. Yankielowicz, Instantons and confinement, Nucl. Phys. **B146**, 256 (1978).

[11] G. Mack and V. B. Petkova, Comparison of lattice gauge theories with gauge groups Z_2 and SU(2), Ann. Phys. (N.Y.) **123**, 442 (1979).

[12] G. Mack, Predictions of a theory of quark confinement, Phys. Rev. Lett. **45**, 1378 (1980).

[13] G. Mack and V. B. Petkova, Sufficient condition for confinement of static quarks by a vortex condensation mechanism, Ann. Phys. (N.Y.) **125**, 117 (1980).

[14] G. Mack and E. Pietarinen, Monopoles, Vortices and Confinement, Nucl. Phys. **B205**, 141 (1982).

[15] E. Tomboulis, 't Hooft loop in SU(2) lattice gauge theories, Phys. Rev. D **23**, 2371 (1981).

[16] M. Faber, J. Greensite, and Š. Olejník, Casimir scaling from center vortices: Towards an understanding of the adjoint string tension, Phys. Rev. D **57**, 2603 (1998).

[17] D. Neudecker and M. Faber, Thick-Center-Vortex-Model and the Coulombic Potential, *Proc. Sci.*, CONFINEMENT2008 (2008) 182.

[18] S. Deldar and S. Rafibakhsh, Short distance potential and the thick center vortex model, Phys. Rev. D **80**, 054508 (2009).

[19] A. Ahmadi and S. Rafibakhsh, Trivial center element and Coulombic potential of the thick center vortex model, Ann. Phys. (Amsterdam) **376**, 145 (2017).

[20] S. Deldar and S. Rafibakhsh, SU(4) String tensions from the fat-center-vortices model, Eur. Phys. J. C **42**, 319 (2005).

[21] S. Deldar, Potentials between static SU(3) sources in the fat-center-vortices model, J. High Energy Phys. 01 (2001) 013.

[22] S. Deldar and S. Rafibakhsh, Confinement and the second vortex of the SU(4) gauge group, Phys. Rev. D **76**, 094508 (2007).

[23] S. Deldar and S. Rafibakhsh, Removing the concavity of the thick center vortex potentials by fluctuating the vortex profile, Phys. Rev. D **81**, 054501 (2010).

[24] J. Greensite, K. Langfeld, Š. Olejník, H. Reinhardt, and T. Tok, Color Screening, Casimir scaling, and domain structure in G(2) and SU(N) gauge theories, Phys. Rev. D **75**, 034501 (2007).

[25] L. Lipták and Š. Olejník, Casimir scaling in G_2 lattice gauge theory, Phys. Rev. D **78**, 074501 (2008).

[26] B. H. Wellegehausen, A. Wipf, and C. Wozar, Phase diagram of the lattice G_2 Higgs model, Phys. Rev. D **83**, 114502 (2011).
[27] B. H. Wellegehausen, A. Wipf, and C. Wozar, Casimir scaling and string braking in G_2 gluodynamics, Phys. Rev. D **83**, 016001 (2011).
[28] S. Deldar, H. Lookzadeh, and S. M. H. Nejad, Confinement in G(2) gauge theories using the thick center vortex model and domain structures, Phys. Rev. D **85**, 054501 (2012).
[29] S. M. H. Nejad and S. Deldar, Role of the SU(2) and SU(3) subgroups in observing confinement in the G(2) gauge group, Phys. Rev. D **89**, 014510 (2014).
[30] S. M. H. Nejad and S. Deldar, Contributions of the center vortices and vacuum domain in potentials between static sources, J. High Energy Phys. 03 (2015) 016.
[31] K. Holland, P. Minkowski, M. Pepe, and U. J. Wiese, Exceptional confinement in G(2) gauge theory, Nucl. Phys. **B668**, 207 (2003).
[32] S. Rafibakhsh, Effect of the SU(4) group factor in the thick center vortex potentials, Phys. Rev. D **89**, 034503 (2014).
[33] A. Das and S. Okubo, *Lie Groups and Lie Algebras for Physicists* (World Scientific, University of Rochester, New York, USA, 2014), DOI: 10.1142/9169.
[34] R. Feger and T. W. Kephart, LieART-A Mathematica application for Lie algebras and representation theory, Comput. Phys. Commun. **192**, 166 (2015).
[35] F. Bastianelli and P. van Nieuwenhuizen, *Path Integrals and Anomalies in Curved Space* (Cambridge University Press, Cambridge, UK, 2006).
[36] L. Frappat, A. Sciarrino, and P. Sorba, *Dictionary on Lie Algebras and Super Algebras* (Academic Press (London), UK, 2000).
[37] R. Slansky, Group theory for unified model building, Phys. Rep. **79**, 1 (1981).
[38] M. Gell-Mann, P. Ramond, and R. Slansky, Color embeddings, charge assignments, and proton stability in unified gauge theories, Rev. Mod. Phys. **50**, 721 (1978).
[39] A. M. Bincer, Casimir operators of the exceptional group F_4: the chain $B_4 \subset F_4 \subset D_{13}$J. Phys. A **27**, 3847 (1994).
[40] J. Patera, Labeling states and constructing matrix representations of F_4J. Math. Phys. (N.Y.) **12**, 384 (1971).
[41] http://www.hepforge.org/downloads/lieart/.
[42] A. J. Macfarlane and H. Pfeiffer, On characteristic equations, trace identities and Casimir operators of simple Lie algebras, J. Math. Phys. (N.Y.) **41**, 3192 (2000).
[43] R. C. King, U(1) factors in branching rules, Physica (Amsterdam) **114A**, 345 (1982).
[44] M. von Steinkirch, *Introduction to Group Theory for Physicists* (University of New York at Stony Brook, New York, 2011).
[45] S. Rafibakhsh and A. Shahlaei, Confinement in F_4 exceptional gauge group using domain structures, EPJ Web Conf. **137**, 13013 (2017).
[46] J. M. Ekins and J. F. Cornwell, Semi-simple real subalgebras of non-compact semi-simple real Lie algebras. 5, Rep. Math. Phys. **7**, 167 (1975).
[47] M. Pepe and U. J. Wiese, Exceptional deconfinement in G(2) gauge theory, Nucl. Phys. **B768**, 21 (2007).
[48] G. Cossu, M. D'Elia, A. DiGiacomo, B. Lucini, and C. Pica, G_2 gauge theory at finite temperatureJ. High Energy Phys. 10 (2007) 100.
[49] A. Maas and Š. Olejník, A first look at Landau-gauge propagators in G_2 Yang-Mills theory, J. High Energy Phys. 02 (2008) 070.
[50] M. Bruno, M. Caselle, M. Panero, and R. Pellegrini, Exceptional thermodynamics: the equation of state of G_2 gauge theory, J. High Energy Phys. 03 (2015) 057.